A Porous Silicon Carbide Ammonia Sensor

Samyuktha Jagarlamudi

Technische Universiteit Delft

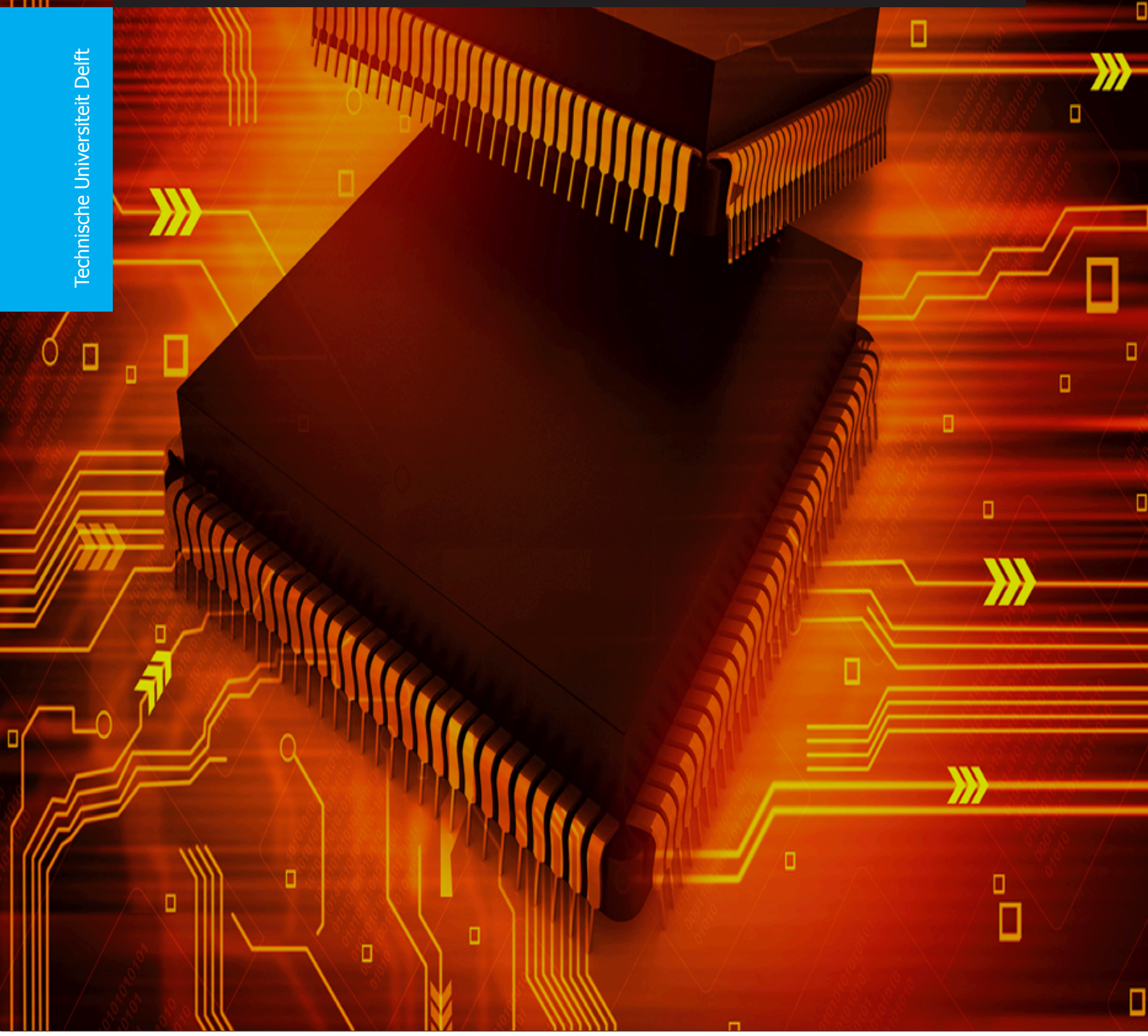

TU Delft Delft University of Technology

Challenge the future

A Porous Silicon Carbide Ammonia Sensor

by

Samyuktha Jagarlamudi

in partial fulfillment of the requirements for the degree of

Master of Science

in Electrical Engineering

Department of Signals and Systems

Faculty of EEMCS

Delft University of Technology

to be defended publicly on Tuesday February 25, 2019 at 13:30 PM.

Supervisor	:	Dr. P.J. French
Thesis Committee	:	Dr.ir. H.W. van Zeijl
		Dr.ir. A. Bossche
		Dr.ir. J.F.L. Goosen(Hans)
Daily Supervisor	:	Dr. G. Pandraud

TU Delft Delft University of Technology

Abstract

Large scale industries like automobile, agriculture and poultry etc.. are in the need of a reliable technology for gas sensors. Till date various types of sensors have been developed for gas applications but the SiC gas sensing has been a recent trend. With increase study in MEMS technology, the SiC material is gaining importance for sensor applications.

Although, Silicon Carbide has been the epitome of research in the field of semiconductors in past couple of years due to its commendable properties and resilience. And being one of most used semiconductor in the field of sensor applications lately, an extensive research is being done and proved that Silicon Carbide is one the best suited sensor material. But very little is known about the possibilities of porous silicon carbide and its applications. Since there is no extensive research available on porous Silicon carbide, this thesis aims at it to show how silicon carbide can be made porous, and the role of it in the gas sensor application.

An in-depth study of the silicon carbide including its features, issues, and possible advantages and disadvantages. A detailed procedure on design and fabrication is presented along with various models and its parameters used to fabricate the sensor device. The design parameters, technical and economic feasibility of the device are discussed using the results from the experiments.

Acknowledgment

When I first set out to take up this thesis, I was excited to work on something that was interdisciplinary and challenging. It did keep me on my toes with new obstacles and concepts at every step which I overcame and successfully could get some results. The months of hard work would not have materialized without the help and support of many individuals whom I wish to acknowledge. I would like to express my sincere gratitude to my supervisor, Dr. Patrick J. French, who trusted me with the freedom to explore various ideas and showed dedicated interest to my progress. I would like to thank him for his supervision, support, and for always being encouraging and motivating. I am indebted to my PhD mentor Manjunath for his unfaltering support, patience and understanding, and supervision. I owe him my sincere thanks for his friendly words of advice and efficacious remarks over multiple fruitful discussions.With the guidance of my supervisors, I have learned to love and respect research for what it is.

I would like to thank Silvana who was instrumental in helping me out with arranging for equipment's needed for my thesis period. When things didn't work or weren't explainable, she was always there to provide advice and guidance on what needed to be done. I am grateful for her constant support.

The lab process would not have been possible without the immense support of Mr. Mario my lab mentor whom I could approach with any doubt and he knew the answers to all things related . For this, I am incredibly grateful and extremely thankful for his efforts and for his patience with me during my journey at EKL.

It was wonderful working with Dr. Henk van Zeijl who was always enthusiastic in answering questions and helping me out with my lab work. His love towards work is contagious. Thank you Henk, your enthusiasm and energy is something I will always look up to. Mr. Greogry despite being a busy man helped me out a lot with my process steps in the lab. Thank you Greogry for helping me even when it wasn't your job and supporting me through my thesis as immensely grateful and indebted for his patience with me and constant support.

I would like to thank all the people from the Else Kooi Lab who have been so friendly and helpful through the thick and thin of my thesis. Thank you Tom, Robert, Koos, Luke,Joost, Lukasz, Hitham, Jia Wei, Violetta, Martijn, Stephan, Vinod. They made my work at EKL fun and were always ready to help.

I am extremely thankful for the friends I made here in Delft, they are not just friends, I would call them family. It was a great experience and having met people from so many cultures, working and growing in this international environment has been a enriching experience. I can proudly say i have friends that I can reach out to when pointed at any place on the World map. They have kept me sane through the tides of my master's journey. I will always cherish my time with them.

Finally, I would like to thank my family, who have made a lot of sacrifices to see me in this position. I am extremely grateful for their constant support, love and care, without which I could not have completed this Masters study.

I hope to have lent a positive experience to everyone around me and I hope that this project serves well for any person who is interested.

Many Thanks,
Samyuktha Jagarlamudi

List of Figures

List of Tables

Contents

List of Abbreviations

Chemical Abbreviation:

ZnO	Zinc Oxide
SiH4	Silane
CH4	Methane
CO	Carbon Monoxide
H	Hydrogen
C	Carbon
CO2	Carbon dioxide
H2SO4	Sulphuric Acid
HF	Hydrofluric Acid
NO	Nitrogen oxide
NO2	Nitrogen dioxide
Pd	Palladium
Pt	Platinum
GaAs	Gallium monoarsenide
Cu	Copper
AgCl	Silver chloride
Ag	Silver
Ti	Titanium
TiN	Titanium Nitride
KOH	Potassium hydroxide

Technical Abbreviation:

SiC	Silicon Carbide
MEMS	Micro-Electro Mechanical Systems
MOSFET	Metal Oxide Semiconductor Field-effect Transistor
SMO	Semiconduvting Metal Oxides
LPCVD	Low Pressure Chemical Vapour Deposition
PECVD	Plasma Enhanced Chemical Vapour Deposition
LED	Ligth Emitting Diode
IR	Infrared Spectroscopy
ppm/ppb	parts per million/parts per billion

SOI-wafer	Silicon-On-Insulator wafer
PEC	Photoelectrochemical Etching
RIE	Reactive Ion Etching

1

Introduction

Section 1.1 gives a brief history of gas sensors and its importance in several applications. Section 1.2 explains the motivation behind this thesis along with the main objective of this project and section 1.3 lists the intended outcomes of the thesis. Section 1.4 outlines the structure of each chapter included, giving a basic overview of what can be expected.

1.1. History

Gas sensors are multifarious in the modern industrial technology. It is being developed and researched on large scale in industry and academia[1]. For each application, a different sensor configuration is usually need to meet the criteria for a particular gas sensing application. An arrayed device, capable of being inexpensively calibrated for a prescribed set of analyte gases, would present an ideal device for a diversity of applications. Due to the hybridization of the nanoporous/microporous silicon medium as the transduction site, we have been able to produce effective individual gas sensors. The gas sensing technology has become significant due to its wide spread application in i) Automotive industry, ii) Industrial production iii) Medical application, iv) Environmental studies etc[2].

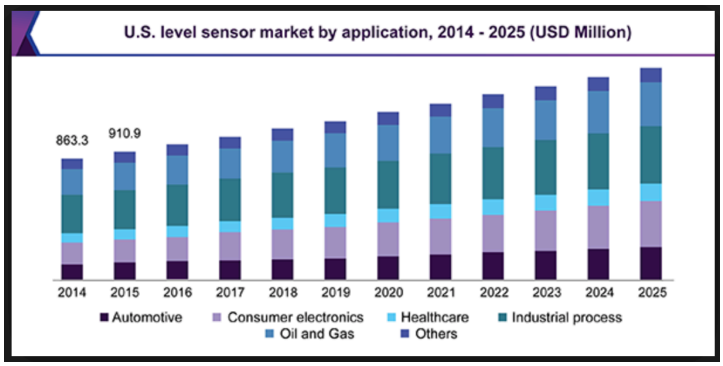

Figure 1.1: Increasing demand for sensor technology from 2014 to 2025

Since, gas sensing/sensors have become an integral part of technology that new materials are being researched for upgrading the sensor world. Following the development the SiC technology over the past couple of years there has been quite significant improvements in the electronic gas sensor device technology and material processing etc.,. Although the literature shows that SiC achieves higher speed, higher power and works at higher temperature. These factors have opened new areas for the application of semiconductor electronics. Despite the added value of such possibilities, the field is noticeably lacking in commercial exploitation of these advances. The reasons behind the limited uptake of SiC are many, the immaturity in both material and processing technology being the key factor[3].

Many of the applications areas of SiC devices are today highly specialized but with relatively small volumes. Due to this aspect of small volume it turns out to be of high cost in terms of production and as such it can also be of a high risk. The perception of SiC being an immature material can counter

balanced with its performance gains that it can offer. This is one of the reasons that the market has been cautious in taking up SiC to a commercial level[4].

1.2. Objective

The main objective of this thesis is to study the properties, effects of Silicon carbide material which is a semiconductor material, along with investigating its use for the sensor technology. Followed by an experimental setup to test its reliability as sensor material using electrochemical etching. The most important aspect of this is to make silicon carbide porous for gas sensing. In which devices are made using silicon carbide as capacitive sensors and measurements are recorded. And, humidity and ammonia gas measurements are carried out to test its sensitivity and selectivity.

1.3. Outcome of thesis

The outcome of this thesis is highlighted as:

- Experimental method to be able to make Silicon Carbide porous and design a device to be used for sensing experiments.
- Understanding the chemistry and material aspects of Silicon Carbide
- Recommendations for porous ammonia sensor design

1.4. Layout

This report will explore various aspects about gas sensing, silicon carbide as a gas sensing material and other parameters that play a part it designing the device and making porous formation in SiC. The chapter 1 gives a brief history and introduction to gas sensing, the main objective, outcomes and the layout of the entire report.

Chapter 2: This chapter deals with an in-depth learning and knowledge about what is chemical gas sensing, types of chemical gas sensors.Furthermore the silicon carbide material is discussed, about its properties, applications etc.. and why is Silicon carbide being used in this experimental thesis.

Chapter 3: In this chapter, the entire fabrication process carried out in the DIMES laboratory EKL is discussed along with challenges faced during the processing. And the design of the electrode and contact opening mask are represented pictorially with brief description. The chapter futher focuses on the experimental set up in the MEMS lab, used for the electrochemical etching of the SiC material and the electrochemistry behind the etching is discussed

Chapter 4: This chapter gives an overview of the results obtained from the processing of the gas sensing device and measurements that are carried out in the process .

Chapter 5: Conclusions and future work is the scope of this chapter, where the end results conclusions are reported along with potential inputs for the further work on this gas sensing device .

[**?**] [**?**]

2

Litrature Study on Gas Sensing and Silicon Carbide as Material

2.1. Gas Sensors

A sensor is a device that receives a signal, either in the form of physical, chemical or biological and converts into electrical signal. Depending on the input signal, there are various types of sensors, such as optical, electrical, thermal, mechanical, chemical, and so on.

But a chemical sensor is a device which converts a chemical signal into an electrical one. In a chemical sensor (which consists of two parts, the sensing element and the transducer), the sensing element changes the chemical properties in accordance with the ambient and the transducer transforms this chemical change into electrical one. The gas sensors are included in chemical sensors group. So gas sensor is a device which can detect the presence of various toxic and combustible gases present in the environment[5]. The interaction between the test gas and the sensing surface can be detected by the measurements of change in resistance, capacitance, work function, mass, optical characteristics etc.

There are a numerous use of these gas sensors. Particularly, using these gas sensors human beings can be saved from potential dangers. Hence the gas sensors play important roles in various sectors, which include industry, medical, environmental applications, and domestic applications for monitoring toxic and flammable gases. Some of the important applications of gas sensors are summarized below:

2.1.1. Solid State Gas Sensors

Acoustic wave gas sensors:

These sensors have a chemically selective sensing layers which are coated on piezoelectric substrates, such as quartz, ZnO etc. which can act as resonant elements. When these sensing elements are exposed to any test gas environment, the adsorption of gaseous species on the sensing layer results a mass loading in the resonant element leading to a reduction in the resonant frequency[6].

As a result there is a shift in the value of the frequency, which can be detected and measured accurately. A variety of gases can be detected using these sensors depending on the type of the sensing layers used. However, the main disadvantages of these sensors are the requirement of high frequency and very complex circuit for its operation[7].

Metal-oxide-semiconductor field effect transistor (MOSFET) gas sensors:

These sensors consist of a source, drain and gate. Usually the gate is a metal (catalytic metals such as Pd, Pt etc.) contact which acts as the sensing element. Next to the gate there exist an oxide insulator and at the opposite side of the insulator there exist a semiconductor. The source provides and the drain collects the charge carriers (may be holes or electrons depending on the type of the MOSFET).

The amount of charge carriers (or current) can be controlled by controlling the electric field in the semiconductor. The change in current, results from the change in work function of the metal and semiconductor, in presence of the test gas. Hence the efficiency of MOFET gas sensors depends on the type of metal used and the operating temperature (as the carriers in a semiconductor changes with the temperature). There are a number of advantages of these sensors as they are small in size and can be reproduced easily. However, these sensors are mostly used to detect H2 gas.

Optical gas sensors:

In optical gas sensors the sensing layer is usually a polymer based layer. Upon exposure of these sensors to a test gas environment, results in the change in optical parameters (e.g. refractive index, absorption coefficient, etc.), due to the interaction of the test gas with the sensing layer[7].

These sensors work efficiently and offer faster response. It has wider gas sensing capability when combined with Raman or IR spectroscopy and are environmental friendly as no electric requirement is needed. However, these sensors have often poor life time [8].

Electrochemical gas sensors:

Electrochemical gas sensors consist of two electrodes (one sensing electrode and another reference electrode) separated by a thin layer of electrolytes. These electrodes are made up of noble metals or gold which can catalyze the test gas and the electrolytes carries the charges across the electrodes. When these gas sensors are exposed to the test gas environment, the gas is either oxidized or reduced at the sensor electrode and the resulting current is measured. From the value of the measured current the concentration of the test gases can be estimated[8][9].
Electrochemical sensors are divided into three types; amperometric, potentiometric, and conductometric gas sensors.

- In potentiometric gas sensors the generated signal is independent of the size of the sensor, whereas in amperometric gas sensors the current is proportional to the size of the electrode and hence sensors having smaller size produce lesser current.
- The primary uses of the potentiometric gas sensors are oxygen sensors or λ-sensors, which are used to monitor the air/fuel ratio in automotive combustion engines. The air/fuel ratio is determined by comparing the partial pressure of oxygen in the exhaust and that in the ambient air.
- In amperometric gas sensors a zero oxygen concentration is maintained at the cathode by applying a high voltage externally. Now the diffusion of oxygen from cathode to anode determines the efficiency of these sensors.

Chemi-resistive gas sensors:

In chemi-resistive gas sensors the sensing layer can be either of a variety of materials, like semiconducting metal oxides (SMO), composites, carbon nanotubes, polymers etc.. The principle of operation of these sensors is primarily based on the changes in resistances upon exposure to the target gas.
Though the polymer based sensors offer reasonably good sensitivity, however, the poor life time of

these sensors limits their use . On the other hand, the SMO based sensors are useful, due to their low cost, ease of preparation, high sensitivity, and long term stability. However, the poor selectivity and higher operating temperature sometimes limits their use in different applications.

Among all the gas sensing materials, SMO based resistive gas sensors (e.g. SnO2, ZnO, WO3 etc) have been extensively studied due to their lower cost, ease of synthesis and simplicity in use.

2.2. Semiconductor Material : Silicon Carbide

As studies are being done SiC has established itself as an important semiconductor material.It is a leading material for the development of microelectrochemical systems (MEMS) that operate under harsh conditions. The high temperature capability of SiC resulting from its large band-gap, extreme hardness, high Young's modulus, chemical inertness and strong radiation tolerance make SiC an exceptional material to be used in combustion and spacecraft electronic systems[3][10]. Also Si and GaAs and other semiconductors fail to show such properties, making SiC the most researched material for applications on a wide range. Along with these properties of SiC its high sublimation temperature conditions and reliable operation of devices at temperatures above 500^0 C[11].

Some of the applications that silicon carbide is being considered and researched on are[12]:

- Spacecraft : Spacecraft with high temperature, radiation hard silicon carbide electronics will enable challenging missions in both the inner and outer solar system. Compact and lightweight silicon carbide high efficiency power electronics will additionally reduce spacecraft launch weights and increase satellite functional capacities.

- Aircraft : Silicon carbide electronics and sensors that could function mounted in hot engine and aerosurface areas of advanced aircraft would enable substantial weight savings, increased jet engine performance, and increased reliability.

- Power : Superior silicon carbide power electronics will increase the efficiency and reliability of the public electric power distribution system, and will prove vital to the increasing use of renewable solar and wind power resources.

- Automotive : Silicon carbide will enable more practical electric vehicles and other tranportation systems by means of vastly improved power electronics. Silicon carbide high temperature electronic sensors and controls on conventional automobile engines will also enable cleaner burning, more fuel efficient cars.

- Energy Production : As energy production demands continue to drive drilling towards greater depths and faster drilling rates, drill-head operating temperatures are expected to rise beyond the operational limits of silicon. SiC sensors and circuits are expected to enable critical telemetry capability at drill-head temperatures greater than 300 C expected in future drilling of energy production wells.

- Communication : Silicon carbide based microwave electronics can function at large power densities and high temperatures offering significant improvements to wireless communications and radar.

2.2.1. Silicon Carbide structure:

Silicon, like carbon can form giant covalent networks. Also, SiC exists in a similar structure to diamond.

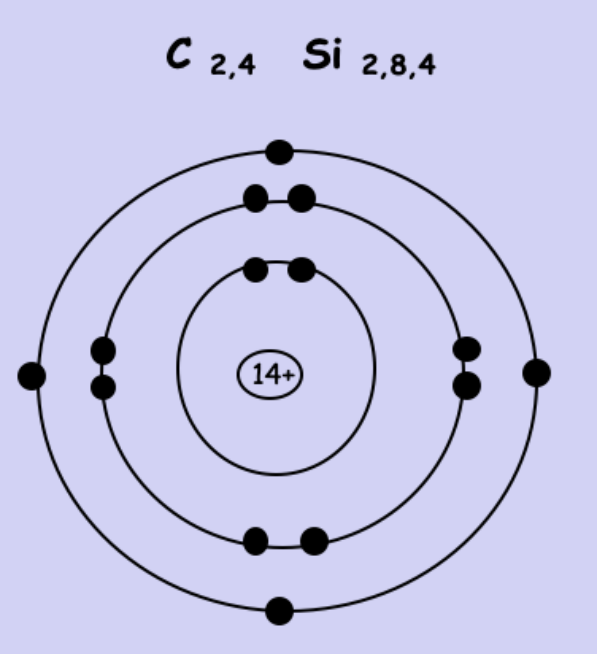

Figure 2.1: Silicon Carbide orbit with atoms

Silicon like carbon needs four more electrons to achieve a stable electron arrangement.The Outer Shell SiC structure looks like the figure below:

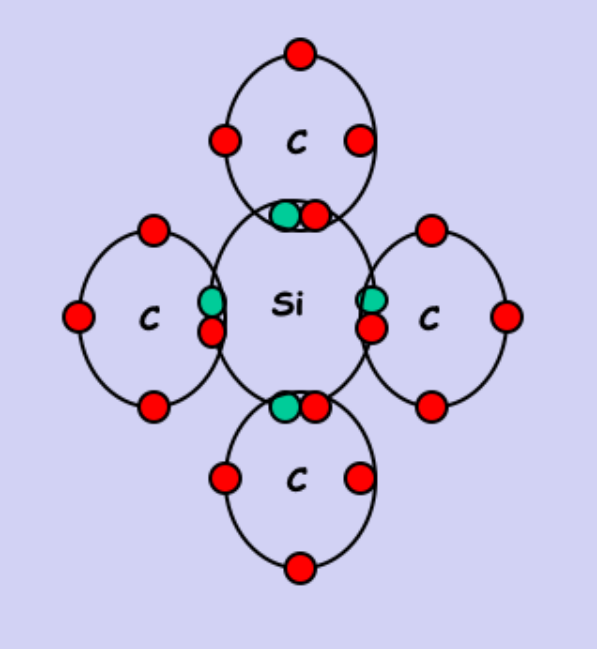

Figure 2.2: Silicon Carbide and Carbon atoms covalent bond structure

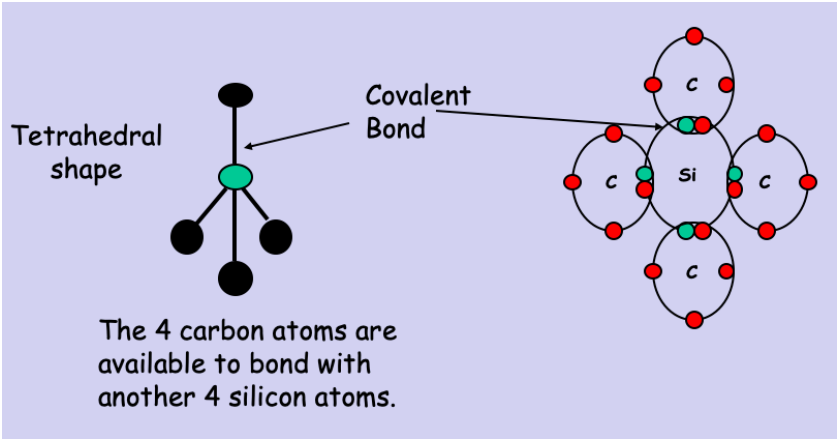

Figure 2.3: Covalent Network Compound

2.2.2. Mechanical Theory:

Residual Stress:

In addition to its resistance to stress-induced deformation as characterized by its Young's modulus, thin films contain an innate biaxial stress as a result of deposition conditions and post-deposition annealing. This stress yields a bulk net force that can be compressive exhibiting tensile stress generally being selected for microfabrication due to their forming readily modeled, taught surfaces when suspended. Depending on device structure and geometry, mechanical performance may depend on stress, Young's modulus, or a combination, so both of these metrics are characterized for a-SiC films in order to provide device designers with flexibility in selecting an optimum deposition recipe tailored for a given application.

Young's Modulus:

Young's modulus is a measure of a material's stiffness and has its origins in Hooke's Law, which relates the force on a spring and its displacement as shown below:

$$F = -k * x \tag{2.1}$$

where F is the force applied to the spring, k is the spring constant, and x is the distance the spring has been displaced from its typical length. This equation indicates that an increasing amount of force is required to elongate a spring the more it is stretched. Additionally, springs with a higher spring constant require more force than springs with lower spring constant to elongate them to the same distance. This equation describes a one-dimensional system and is analogous to three-dimensional model from which the Young's modulus is determined.[13]

In the three-dimensional system, the concepts of stress and strain are introduced in order to fully describe the behavior of a given material under an applied force. Stress , which is analogous to force in the one-dimensional system, represents an force on a section of material, and is produced either by internal molecular interactions or transmitted through the material from an external stimulus. The formula for computing stress is shown below:

$$\sigma = F/A \tag{2.2}$$

where σ is stress, F is applied force, and A is the cross sectional area normal to the applied force vector. This indicates that stress has units of pressure, and is represented in this work in units of Pascals (Pa = N/m^2).

As a result of this applied force and stress, a sample of material will exhibit elongation along the

direction of the force, which is defined as strain (ϵ) and is calculated as shown below[14]:

$$\epsilon = \delta L/L \tag{2.3}$$

Based on this equation, strain is dimensionless and is analogous to x in equation 1, and expresses the change in a materials length(Δ L) with respect to its original length (L)when a force is applied. These metrics for calculating stress and strain are summarized in

The Young's modulus relates an applied stress to its resulting strain for a given material using the equation below:

$$E = \sigma/\epsilon \tag{2.4}$$

where E is the Young's modulus, σ is stress, and ϵ is strain. The Young's modulus,which has units of pressure (Pa), is analogous to the spring constant k in the onedimensional model, providing a metric for the resistance to elongation that a material exhibits under an applied force or stress. Materials with a high Young's modulus areregarded as having high stiffness and demonstrate small strain for a given magnitude of stress. Similarly, materials with low Young's modulus will provide a higher strain for the same applied stress. Table below contains a summary of values of Young's modulus for several common materials and materials used in microfabrication.

Material	Young's Modulus(GPa)	Reference
Steel	200	[15]
Concrete	17	[15]
Rubber	0.1	[15]
Gold	79	[16][17]
Chromium	280	[18]
Nickel	200	[16][17]
Silicon(crystalline)	160	[19]
Si_3N_4	150	[20]
sc-SiC(3C)	401	[21]
poly-SiC(LPCVD)	399	0[22]
a-SiC(PECVD)	196	[22]
a-SiC(sputtered)	231	[23]
SiO_2(Crystalline)	80	[24]
Al_2O_3(Crystalline)	380	[25]

Table 2.1: Summary of typical Young's moduli for common materials

Possion's Ratio:

When a material exhibits stress-induced strain, it often produces a corresponding reduction in cross-sectional area. Although the Young's modulus characterizes the material's resistance to strain along the direction of an applied stress, it does not take this effect into consideration. The Poisson's ratio (v) was defined to address this effect, and is defined as shown in the equation below:

$$v = \frac{-\epsilon_t}{\epsilon_a} = \frac{-\Delta T/T}{\Delta L/L} \tag{2.5}$$

where ϵ_t is transverse strain, ϵ_a is axial strain, T is initial material thickness, is the change in thickness due to strain, L is initial length, and ΔL is change in length due to strain. This metric accounts for deformation of a sample under applied stress, and is typically in the range of 1.0 – 0.5 for elastic materials[14]. A summary of typical values of Poisson's ratio for various materials in the table below:

Material	Possion's Ration	Reference
a-SiC(PECVD)	0.23	[23]
Poly-SiC	0.17	[20][26]
sc-SiC(3C)	0.201	[27]
Si_3N_4(LPCVD)	0.28	[28]
SiO_2(Thermal)	0.17	[29]
<100>silicon	0.17	[30]
Gold	0.44	[15]
Chromium	0.21	[15]
Nickel	0.31	[15]
Rubber	.48	[15]
Steel	.265	[15]

Table 2.2: Summary of typical Poisson's ratios for various materials

Since Silicon carbide has high thermal conductivity, hardness, low linear thermal expansion etc.. these parameters are expressed in numbers below:

Hardness[31]

Mohs scale	Between 9 and 10
Knoop scale	25,000 to 30,000 N/mm^2

Thermal Conductivity[31]

20^o	0.41 W/cm^oC
1000^o	0.21 W/cm^oC

Linear Thermal Expansion[31]

$20 - 1000^o$ C	$5.1 * 10^{-6}/^o$ C
$20 - 2000^o$ C	$5.8 * 10^{-6}/^o$ C

Specific Heat[31]

25^o C	$0.67J/g^oC$
1000^o C	$1.26J/g^oC$
Specific density	$3.21g/cm^3$
Bluk density	$0.5 - 1.7g/cm^3$

Melting Point

Silicon carbide does not melt, but dissociation starts at about 2.300°C [31]

2.2.3. Chemical Theory

Silicon carbide will not dissolve in acids or in bases, but is easily attacked by alkaline melts and by most metal and metal oxide melts. This is because the fundamental structural unit of Silicon Carbide is Covelently bonded primary co-ordinated tetrahedron, either SiC_4 or CSi_4. The four bonds directed to the neighbors have a nearly purely covalent character. Thus Silicon Carbide exists in a similar structure to Diamond. Since the covalent bond or lattice is very difficult to break, silicon carbide comes a hard substance and chemical inert due to this chemical structure that exists in it.

Further looking into the covalent bond strength it depends on the energy required to break it. The C-Si single bond energy is 360, which is a high bond energy for the covalent to be broken. Although triple and double covalent bonds have much higher bond energy and are much difficult to be broken than single bond like c-Si. Accordingly the bond length decreases based on the number of bonds.

Amorphous Silicon Carbide

Amorphous networks still raise numerous questions concerning the physical basic understanding. Especially amorphous tetrahedral alloys seem to be a very complex system. In the case of a compound material, as it is the case for SiC, the situation gets even more complicated.As far as we know from literature[32][33][34] the deposition method, the precursor gases, the hydrogen content and the C/Si fraction have a very strong influence on the network of an amorphous material. Explations on stoichiometric amorphous SiC layers which were deposited by plasma enhanced chemical vapour deposition from silane (SiH4) and methane (CH4).

bond	length [10^{-1} nm]	bond	length [10^{-1} nm]
C–C	1.54	C=C	1.33
C–H (sp^3)	1.09	C=C (graphite)	1.42
C–Si	1.87	C≡C	1.21
Si–Si (in c-Si)	2.35	Si–H	1.48

Figure 2.4: SiC relevant bonds and bond lengths.

First of all it can be stated that amorphous tetrahedral alloys will be more disordered than e.g. amorphous silicon since chemical disorder is added to the inherent structural disorder. These structural disorders will be even more pronounced if the coordination geometries of the two atoms are different. This is especially the case for increasing difference in bond length. From the ratio of the covalent radii rC/rSi=0.66 (see figure 2.5) we can conclude that the network models, which have been developed for amorphous silicon, are not suitable to describe amorphous SiC networks. They are expected to be much more disordered. Silicon cannot form homo nuclear pπ-bonds. If carbon atoms form homo or hetero nuclear p-bonds in the alloy (isolated double or triple bonds or resonant - bonding systems) structural disorder will increase considerably.[34]

atom	radius [10^{-1} nm]	electronegativity
C	0.77	2.50
Si	1.17	1.74
H	0.28	2.20

Figure 2.5: Covalent radii and electronegativity of the atoms appearing in the SiC network

For a statistical distribution of atoms in the alloy, there will always be some homo nuclear bonding between majority atoms. Since C-C bonds are thermodynamically more stable than Si-Si and Si-C bonds, it is probable to find C-C bonds already in a material with a C/Si fraction slightly higher than 1. At higher carbon concentrations clusters may be formed which are expected to contain graphitic configurations.

If we consider a continuous random network, there must be a maximum disorder somewhere between pure amorphous silicon and a pure amorphous carbon network. Since the Si-Si and the C-C bonds stability are different this maximum is not to be expected at a ratio C/Si of 1. During film deposition, the amorphous network relaxes, especially at higher temperatures, in order to minimise the free energy. Nevertheless, a residual distortion of coordination geometry always remains in an amorphous network. This residual distortion will be different for carbon and silicon atoms since the coordination behaviour of carbon is much more flexible.

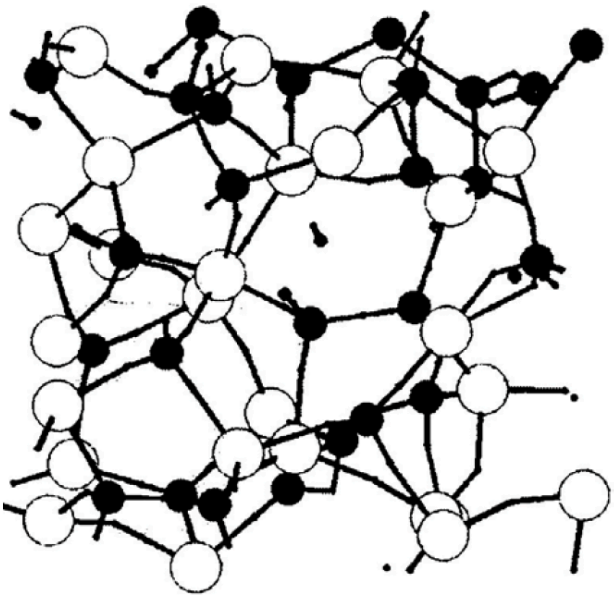

Figure 2.6: Amorphous Silicon Carbide structure

Hydrogenated SiC

When we grow SiC layers from methane and silane at temperatures below 600°C, a significant amount of hydrogen will be found in the amorphous network. The C-H bonds are much more stable than the Si-H bonds which should have consequences for the thermal stability of the films with respect to hydrogen effusion. Furthermore carbon atoms are expected to be more hydrogenated than silicon atoms. Due to the different electronegativities of silicon and carbon (see figure 2.7), Si-H bonds are strengthened if the silicon atom is bonded to a carbon atom (on the other hand the C-H bond is weakened).

	H	C	Si
H	436	416	323
C		356	301
Si			226

Figure 2.7: Bond energies in KJ/mol at 25 degree C

2.3. SiC-based Gas sensors

The most common structure used for detection of gas species in silicon carbide technology is the capacitor with a catalytic metal contact. The dielectric layer allows these devices to operate at temperatures more than 900-degree C by separating the metal from silicon carbide[3]. Gas molecules incident on the catalytic metal decompose and form a charged layer on the surface of the dielectric. This charged layer causes a change in the carrier concentration in the silicon carbide directly underneath the contact.

For hydrogen and hydrogen-containing molecules, the hydrogen atoms can diffuse easily through thick or dense catalytic contacts to form the charged layer. This decomposition occurs at temperatures above 150 degree C and occurs in the sub-millisecond time scale. This high response speed makes silicon carbide sensors suitable for the detection of gas species in rapidly varying environments, such as close to the manifold region in car exhausts, unlike the conventional ceramic based sensors, which have a response time in the region of 10 s under these conditions . The suitability of deployment in car exhausts is further exemplified by the ability of these devices to function over a wide temperature range, unlike ceramic devices' which makes them suitable for cold start applications[35].

For larger gas molecules it is shown that artificially increasing the porosity of the metal contact increases the sensitivity to gases such as CO, butane and No while that of hydrogen is unchanged.

The measurements of gas concentration are performed by measuring the change in voltage required to maintain a constant capacitance. This method has an advantage over measuring the change in capacitance at constant voltage, as this avoids problems with the trapping and detrapping of carriers at the silicon carbide/dielectric interface and thus avoids problems with hysteresis in the sensor output[10].

Another method to the measurement of gas concentration is in the use of the leakage current through the capacitor. This uses a simplified measurement than capacitive measurement. Also, the sensitivity of this measurement technique is not dependent on the gate voltage applied.The sensitivity of catalytic sensor to a gas is determined by both the choice of the metal and the temperature of the operation.However, these sensors are sensitive to a variety of gases and not uniquely to a single gas in general.

Alongside, high temperature piezoresistive pressure sensors have been demonstrated in SiC, but suffer from a significant temperature dependent piezoresistivity and variation in contact resistance that can severely degrade sensor performance as temperatures increase.Capacitive sensors are more tolerant of contact resistance variation and devices with stable operation at 500-600°C have been built using crystalline and polycrystalline SiC films. Unfortunately, these films require deposition temperatures over 900°C. Such high processing temperatures make these films incompatible with thermally sensitive substrates and metalized devices. Conversely, amorphous SiC (a-SiC) can be deposited at temperatures between 200-350°C through plasma enhanced chemical vapor deposition (PECVD), making it a more viable option. Moreover, a-SiC is an electric insulator that has low diffusion constants and resists alloying[10].

These properties have resulted in a-SiC being primarily used as an etch mask for Si micromachining as well as an inter-metal dielectric and diffusion barrier, however, little is known about its mechanical and electrical properties at high temperatures and under cyclic loading. Nevertheless, a-SiC has demonstrated advantageous material properties that, coupled with its low-temperature deposition make it especially attractive for the development of an integrated wireless capacitive sensor platform such as shown in Figure, and to the knowledge, this work is the first of its kind to investigate its mechanical properties at temperatures above 500°C[11].

2.4. Porous Silicon

SiC is a very hard and stable material. It exists in many different modifications.Only a few experimental results are available and many of them have not been sufficiently reproducible.One reason is that reliable single crystals (mostly as thin layers on Si) have become available only in the last two decades. At first sight one may expect anodic behavior similar to that of Si. However, in contrast to Si, the anodic current at a p-type SiC electrode in H_2SO_4 was found to remain stable and did not essentially decrease with polarization time, and a white SiO_2 film was formed after prolonged polarization. The head space analysis of gaseous products revealed CO and CO_2 in a ratio close to 1 : 1. The formations of these products were explained by an eight-hole process and a six-hole reaction which proceed at the same rate, both being given by: Since the oxide does not limit the interfacial current it was concluded that it is very porous. The oxide is very soluble in HF so that SiC can be etched which is important for the production of devices. The anodic decomposition of SiC was also studied in concentrated HF solutions. Since several decades it is known that n- and p-type silicon can be made porous at the surface by anodic etching in HF solutions under conditions where Si is dissolved in its divalent state. Experts in this field expected for a long time that this phenomenon would occur only at silicon because

of its special dissolution properties. Meanwhile, other semiconductors have been made porous such as SiC. Pore sizes (diameter and depth) ranging over many orders of magnitude, are reported. They are mainly discussed in terms of micro and macro pores.

Although Porous Silicon has been researched for past two decades for sensor applications for its luminescence properties, large surface area etc. These porous silicon sensors have been used widely for a lot of applications.Some are mentioned below[36]:

Application area - Role of porous silicon - Key Properties[36]

- Optoelectronics - LED, Waveguide, Field emitter, Optical memory - Efficient Electroluminescence, Tunability of refractive, Hot carrier Emission, Non linear properties
- Micro-optics - Fabry-Pérot Filters, Photonic bandgap structures, All optical switching - Refractive index modulation, Regular macropore array, Highly non-linear properties
- Energy conversion - Antireflection coatings, Photo-electrochemical cells - Low refractive index, Photocorrosion cells
- Environmental monitoring - Gas sensing - Ambient sensitive properties
- Microelectronics - Micro-capacitor, Insulator layer, Low-k material - High specific surface area, High resistance, Electrical properties
- Wafer technology - Buffer layer in heteroepitaxy, SOI wafers - Variable lattice parameter, High etching selectivity
- Micromachining - Thick sacrificial layer - Highly controllable etching
- Biotechnology - Tissue bonding, Biosensor - Tunable chemical, reactivity Enzyme immobilization

The value of PSi gas sensor technology has given results from a combination of[37]:

- Its sensitivity and short recovery time
- Its operation at room temperature as well as at a single, readily accessible, temperature with an insensitivity to temperature drift
- Its potential operation in a heat-sunk configuration allowing operation to a surface temperature of 80-degree C even in highly elevated temperature environments.
- Its ease of coating with diversity of gas selective materials to form sensor arrays.
- Its low fabrication, low cost and ease of rejuvenation after contamination
- Its low-cost operation and ability to rapidly assess false positives by operating the sensor in a pulsed gas mode.

As seen, porous silicon has some commendable advantages and wide range of uses, it still has some slight drawbacks with its material structure. And the research on Silicon Carbide and it's highly suitable properties as a semiconductor device has made it more popular for porous sensor material than porous silicon in general. Porous SiC (pSiC) can be prepared by metal assisted photoelectrochemical etching , which in contrast to conventional anodization of SiC, is capable of producing uniform porous layers. In this approach a noble metal like Platinum (Pt) is deposited on the SiC surface, serving as local cathode. When the sample is immersed in an etching solution containing an oxidizing agent and hydrofluoric acid, a charge transfer occurs with electrons flowing from the SiC substrate via the Pt/SiC interface to the etching solution. Simultaneously pSiC forms at the bare SiC surface. Recent experiments have shown that reliable etching can be achieved by decreasing the contact resistance at the Pt/SiC junction[37].

2.5. Ammonia sensors

Ammonia is a natural gas that is present throughout the atmosphere. There are many ways to detect ammonia. High concentrations of ammonia can be detected easy due to its very pungent smell, and the human nose is very sensitive to ammonia.But to quantify or determine ammonia in low concentrations of ammonia, the human nose fails. However, in many occasions the concentration of ammonia must be known. Two of most important producers of ammonia are Automotive industry and Chemical industry [2].

1. The automotive industry is interested in measuring ammonia for three reasons.

- First reason being the exhaust gasses are monitored because they form the major part of gaseous pollution in urban sites. As ammonia exhaust is associated with airborne particulate matter. Ammonia emissions have been measured up to 20 mg/s or up to 8 ppm ammonia in exhaust gas[38][39].
- Second reason being interested in detectors for atmospheric pollution like ammonia is air quality control in the passenger compartment[38].
- And the third reason for ammonia sensors in automotive area in NOx reduction in diesel engines. Modern diesel engines operate at high air-to-fuel ratios that result in an excess of oxygen in the exhaust gas, resulting in large concentrations of NO and NO2[40].

The currently used ammonia sensors have detection limits in the order of a few ppm [30] and a response time about 1 minute. Because measurements are performed in exhaust pipes, the sensor should be able to withstand elevated temperatures.

2.Chemical industry is another ammonia producing factor. The production of ammonia by chemical industries was initiated by the demand for an inexpensive supply of nitrogen to produce nitric acid, a key component of explosives. Today it is being used in agriculture sector as fertilizers. Another substantial part is used in refrigeration due to its ability to cool below 0. Since the chemical industry uses ammonia in its pure form and is widely required it can be life-threatening and thus ammonia detectors are in high demand.[41][42]

Existing Ammonia Sensing principles:

There are many principles for measuring ammonia. A different sensor is used in the exhaust pipe of automobiles than for measuring ultra low concentrations of ambient ammonia for environmental monitoring. Some of the frequently used commercial ammonia detectors are discussed below.

1. Metal-oxide gas sensors - The metal-oxide gas sensor model is based on metal-oxide flims which consist of large number of grains, contacting at their boundaries[43]. The electrical behaviour is governed by the double Schottky potential barriers at the interface. The height of the barrier determines the conductance. These sensors when exposed to ammonia which is chemically reducing agent, co-adsorption and interaction between the gas the oxygen results in oxidation of the gas at the surface. Which in turn reduces the barrier height[44].

These metal-oxide sensors are not selective to one particular gas; which is a major drawback. These metal-oxide sensors are based on SnO_2 sensors[45]. They are rugged and inexpensive and thus very promising for the developing gas sensors.

2. Catalytic ammonia sensors - The charge carrier concentration in the catalytic metal is altered by a change in concentration of the gas of influence. This change in charge carriers can be quantified using a field effect device, like a capacitor or a transistor[46][47].The selectivity of these sensors depends on parameters like the used catalytic metal, the morphology of the metal layer and the operating temperature. Ammonia field effect transistors, gasfets, using a palladium gate material have been shown, resulting in a detection limit of 1 ppm.

The catalytic reaction of a metal layer with gaseous ammonia can also be used in combination with a solid-state ionconducting material to form a gas-fuelled battery. These gassensing systems are known as chemical cells. The catalytic reaction at the sensing electrode will cause a change in electrode potential. The resulting potential difference between the electrode and a counter electrode, over the conducting layer, is used to quantify the gas concentration. These sensors are commercially available for many different gasses. The lower detection limit is normally in the low-ppm range and the accuracy is limited. A chemical cell for ammonia is presented in literature based on an anion-exchange membrane with a Cu electrode and an Ag/AgCl counter electrode[48].

3. Conducting polymer gas detectors - A third measurement principle for ammonia makes use of polymers. Different materials have been reported, like polypyrrole and polyaniline. The sensing mechanism of polypyrrole films is two-fold: first, there is an irreversible reaction between ammonia and the polymer and, secondly, ammonia can reversibly reduce the oxidized form of polypyrroly[49]. The reduction of the polymer film causesa change in the conductivity of the material, making it a suitable material for resistometric or amperometric ammonia detection. Response times of about 4 min have been shown. The irreversible reaction with ammonia results in an increase in mass in the polymer film[50]. Sensors have been described that detect ammonia using the change in frequency of a resonator, coated with ammonia sensitive polymer. However, the irreversible nature of the reaction causes the sensitivity of the sensor to decrease over time when exposed to ammonia.

Polyaniline proved to be a much more stable conducting polymer material. The polymer is believed to be deprotonated by ammonia, which results in the change in conduction.The lower detection limit of gas sensors based on the two described polymers is about 1 ppm. These sensors are commercially available for measuring ammonia levels in alarm systems.

4. Optical gas analyzers - There are two main optical principles for the detection of ammonia. The first is based on change in the color when ammonia reacts with a reagent. And the second principle based on optical absorption detection.

i. Spectrophotometric ammonia detection- Spectrophotometry is a technique where a specific reaction causes a coloration of an analyte.There are different coloration reactions in use for dissolved ammonia. Best known is the Nessler reaction. This ammonia detection method is readily available and applied frequently for determining the total ammonia concentration in water, e.g. in aquaria where too high ammonia levels can cause fish to die. The Nessler reagent consists of dipotassium tetraiodomercurate(II) in a dilute alkaline solution, normally sodium hydroxide. This reagent is toxic. There is not much literature about quantitative measurements with this reaction, probably because of the disadvantages[51]. Besides the toxicity, a second disadvantage is the formation of the non-soluble reaction product, a basic mercury(II) amidoiodide, making the reaction difficult to implement in a miniaturized detection system.

A second coloration method to measure ammonia concentrations in aqueous solutions is the Berthelot reaction. A combination of ammonia, phenol and hypochlorite results in a blue coloration. This reaction uses less dangerous chemicals and the reaction products are all soluble in water. This makes it a suitable technique for integration in miniaturized analysis systems[52]. One drawback of this technique is the rather slow kinetics of the reactions. This was improved by miniaturization in a flow-through analysis system. The detection limit is about 5μM of ammonia in water or 90 ppb. This technique is still under development in order to lower the detection limit.

To improve the sensitivity, the detection limit of the detector has to be improved. This is done by applying different coloration principles, like thin layers of pH indicator , fluorescent materials that can be used to label ammonia or a combination of the two. A second option is to apply a very sensitive detection principle, like a photon-counting optical sensor or optical waveguide structures to quantify the coloration, resulting in very sensitive, ppt range, ammonia detectors.

ii. Optical absorption ammonia detection- Optical adsorption spectroscopy is used in the most sensitive and selective ammonia detectors for ambient ammonia. Systems with a detection limit of 1 ppb, that do a full measurement in 1 s, have been reported Such systems use a laser and a spectrograph. Light travels through air or an ammonia sensitive layer. The spectrum of the light reaching the detector is influenced by either the gas composition or the material characteristics as a function of the gas composition.

One major drawback of most available ammonia detection principles is the poor selectivity towards ammonia compared to other gasses.

3

Fabrication and Experimental SetUp

The fabrication of the prototype of the gas sensor device was done at DIMES EKL TU Delft. There is a brief explanation of the process involved in fabricating the device below with relevant pictures. It gives an insight into the materials used and processing techniques that are involved with some points that were observed during the fabrication of the device. This section only gives an explanation of why the process steps are done, but a flowchart with will be attached below in the appendix which can be used to follow the steps for further use on this project as it gives information on the steps to be followed during processing accordingly.

3.1. Fabrication Process Steps Specification

3.1.1. Photo-lithography:

The first step in the whole processing is photo-lithography where Coating, Exposure and Development for the wafer is done. The very first process step is Alignment, where these markers are exposed on to the wafer, to be used in further lithography were these alignment markers act as reference to expose other mask for electrode design. The steps for creating these markers involve:

- Coating positive resist on the wafer with recipe Co-3012-noEBR
- Exposing the COMURK mask for alignment marks with an energy of 150 mJ/cm^2
- Development of the alignment markers using the Dev-SP recipe.

The photo-lithography process is repeated twice in the entire process for the gas sensor device fabrication.The 2nd lithography step, again involves coating, baking and developing steps as before but with different recipes and mask.

1.Lithography for Electrodes:

- 1.4 μm SPR-3021 positive resist is coated on the TiN layer deposited earlier during metallisation(explained in the later steps).
- Metal mask EC-2091 image 4 is exposed with 150mJ/cm^2 energy, for the electrode design on the TiN layer.
- For the developing of the electrodes the standard Dev-SP recipe is used again.

The third lithography step is done after deposition of the SiC layer on the electrodes. In this litho step a contact opening mask is exposed to later etch the contact opening through the SiC and land on the

TiN electrodes.This opening acts as the capacitor for the device. The steps are comparable as above:

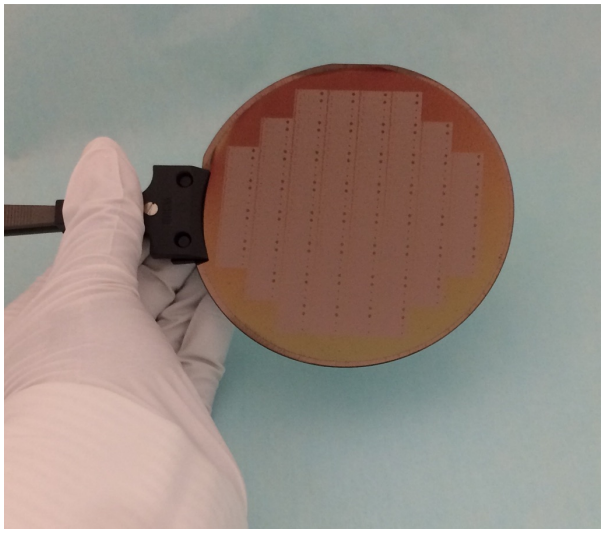

Figure 3.1: Lithography processing on the wafer

2. Lithography for Contact opening:

- 12μm AZ-Syr-9260-positive photo resist is used for coating.**The thickness of the resist is 12μm because there is a 1.7 micrometer layer thick SiC underneath which has to be etched through to open the contact windows.Because the etch rate of SiC is unknown, a thick resist layer was used to etch through the thick SiC layer.**
- Mask EC-2091 image 2 is exposed with 1550mJ/cm^2 energy, for the contact opening.**The energy level for exposure is chosen to be high because of the thick photo-resist used for coating.**
- AZ400K diluted with DI water with ratio of 1:2 was used to develop manually.A total of 5 minutes for each wafer was used for developing.**Since the development is done manually, it is very important to inspect the wafer under microscope to check if all the openings are developed correctly and that there is no residue left.**

3.1.2. Tunnel oxide growth:

- The thermal oxidation process is used for the growth of a ultra-thin oxide layer on a p type-Si wafer as a dirt barrier layer for the implantation to achieve a good electrical contact on the backside of the wafer for the electro-chemical etching.
- After this the p-type Si wafers are processed in furnace C1 with program 300A for a total time of 70 minutes and at temperature of 850^oC.

3.1.3. Ion Implantation and annealing:

- Boron atoms are then implanted at the back side, with an energy of 40 keV and a dose of $1 * 10^16(1.0E16)ions/cm^2$ in the Varian E500HP ion implanter.
- A 165 mins annealing step at 1000°C using program ANNEALN1 in a furnace C2 is then required in order to activate the dopant on the back side.

- Followed by One Nitric Acid Cleaning Cycle – detailed below in the Cleaning Cycle Step and a 0.55 percent HF bath to remove the native oxide are performed.

3.1.4. Metallization:

- Important step in the fabrication of this device is the metallization, which will allow the collection of the charge carriers and the creation of a current through an external circuit at the back end where the Aluminum is deposited on a full surface area.
- Also since Aluminum is a good candidate of electric conduction
- The processing step, involves sputtering Aluminum with 1 percent Silicon is deposited on the back side of the wafer. A 675nm thickness is deposited at 350 degree Celsius. It is used as an electrical contact since it's a good conductor of electricity and an electrochemical etch is required in the later stages to make the Silicon carbide layer porous.
- Then a layer of TiN (Titanium Nitride) is deposited on the front side the wafer. A 350nm thickness is sputtered using recipe TiN 350nm-350^{o}C at 350 degree Celsius in the Sigma.
- TiN is not as easily attacked by a high Concentration of HF as Aluminum. It only makes the TiN surface rough but there is no literature that shows any kind of attack by HF to TiN. Hence it is used an a electrode material in this process.
- Once the Metallization process is done, the second lithography step is performed for the exposure of the electrode design.

3.1.5. Dry Etching:

An etching step is performed after every litho step. The etch steps are used to transfer, the device structures for the experiments to the deposited layers.

- The etching is done using the Trikon Omega 201 plasma etcher.
- For etching the Aligmnment markers the URK-NPD sequence is used with platen temperature of 20 degree C.
- The TiN electrodes are etched using the $tinti_2$ recipe with platen temperature of 25 degree C. **This recipe has an over etch such that there is no short circuit between the electrodes. The overetch can lead to etching 0f into the layer below, for example in my case silicon below TiN was etched to 350nm. It will not make a difference unless your device needs accurate layers.**
- The last etch step is done after the Sic deposition and litho step where the contact pads are exposed. The recipe for this step is yet to be discovered since it has to be etched through SiC layer of 1.7μm thick.
- **Also, the last etch step is done outside the EKL cleanroom 100 since SiC deposition is done in CR10000 and the PECVD machine that is used is considered to be contaminated. So the etch step is carried out in Kavali Nano lab using the Alkatel etcher.**

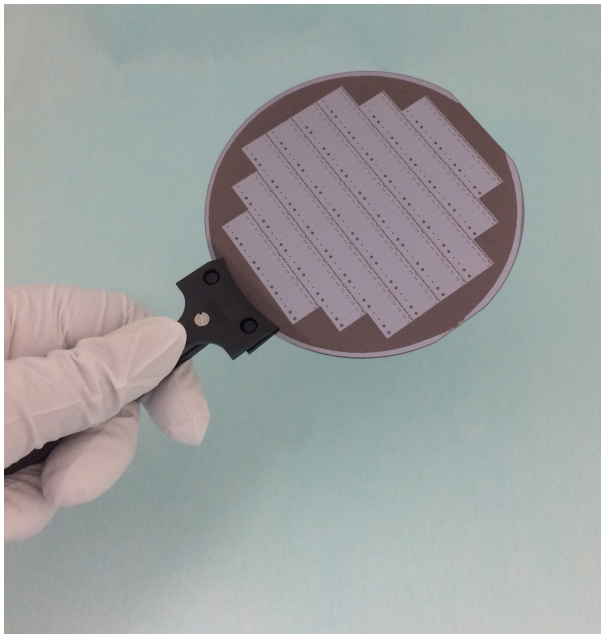

Figure 3.2: Dry etching of the electrodes after Lithography

3.1.6. Amorphous Silicon Carbide Deposition:

- After the electrode patterning on the front side of the wafer is then ready for p-doped SiC deposition on the front side.
- First the wafers are cleaned in the HNO_3 bath before going into the PECVD machine.
- After the cleaning, the wafer is directly loaded to the PECVD chambers – under vaccuum – inorder to avoid the growth of a native oxide in the air environment. The deposition of 1.7μm of a-SiC is done at 180°C with silane (SiH4) and methane (CH4) as gas precursors.
- The Si to C ratio is varied for each wafer, in this step two wafers were processed with 50-50 SiC ratio and 70-30SiC ratio. And most importantly p-doped SiC is used.

3.1.7. Cleaning Cycles

- As mentioned above, at several moments during the process, the wafer needs to be cleaned in an acid bath in order to get rid of some particles and residues e.g. resist.
- Cleaning is performed in Nitric Acid and it consists of dipping the wafer during 10 min in a HNO_3 99 percent solution at ambient temperature, followed by 6 min of rinsing in deionized (DI) water, then another 10 min dip in a HNO_3 69 percent solution at 110°C is done followed by 6 min of rinsing in DI water again.
- Finally, a Marangoni cleaning step is performed, consisting of a 4 min dip in a HF 0.55 percent solution, followed by 5 min rinsing in DI water, so as to remove the native oxide.

The device cross-sectional design is attached below to give a summarized overview of how the end device could look.

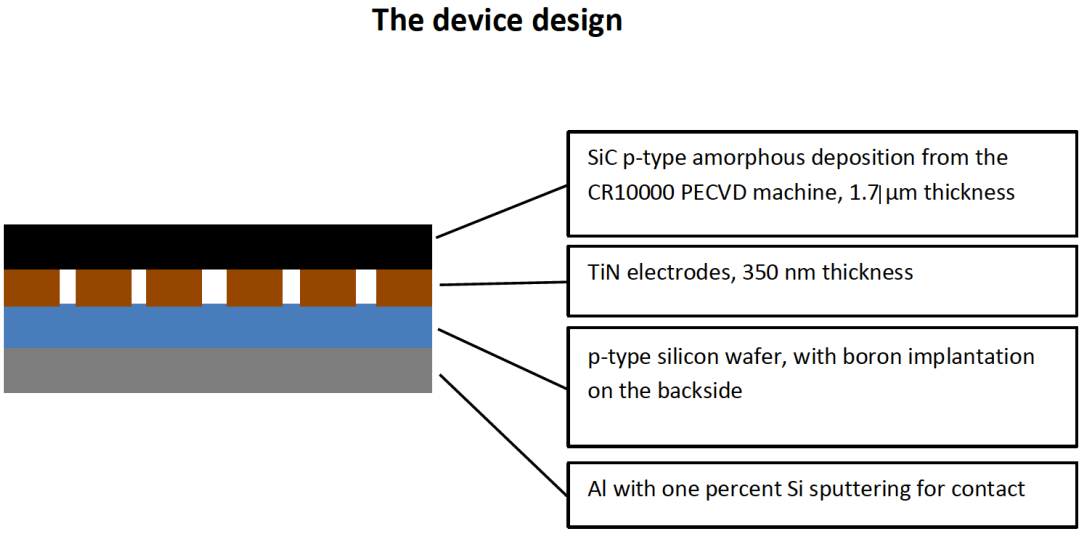

Figure 3.3: Cross-sectional view of the device

3.2. Mask Design of Electrodes and Contact Opening:

A stepper mask with electrode, contact pad design was used in the fabrication of the device. The images of the electrode design are attached below.

In the figure 3.4 below, the zoomed image of the electrode is shown.

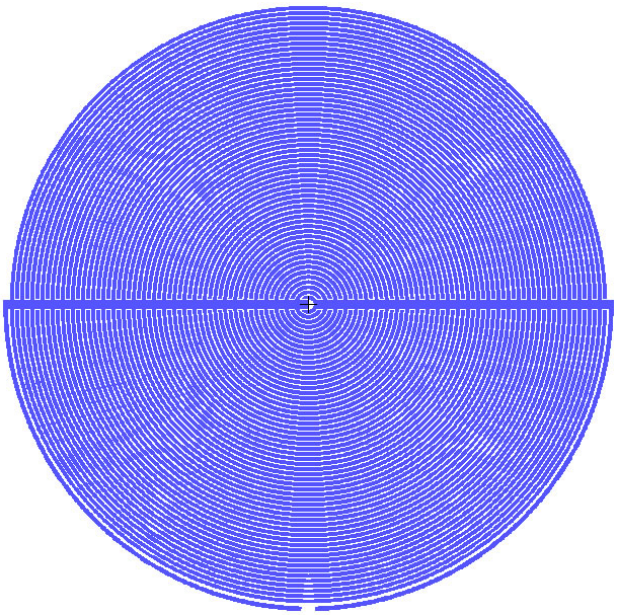

Figure 3.4: Zoomed image of the electrode

The figure 3.5 represents the entire mask design in which the blue rectangular blocks in the bottom which are connected to the black circular electrode design are the capacitor pads. And the non-connected blue square blocks below the capacitors are the heater pads. In this research, only the capacitor pads are used for measurements, since a capacitive based sensor is to be studied and reported.

It can be observed from the figure 3.5 that, there are four electrodes in one block, which consists of 2

big electrodes and 2 small electrodes. The big electrodes are of 1μm thickness and the small electrodes are of 500nm thickness.

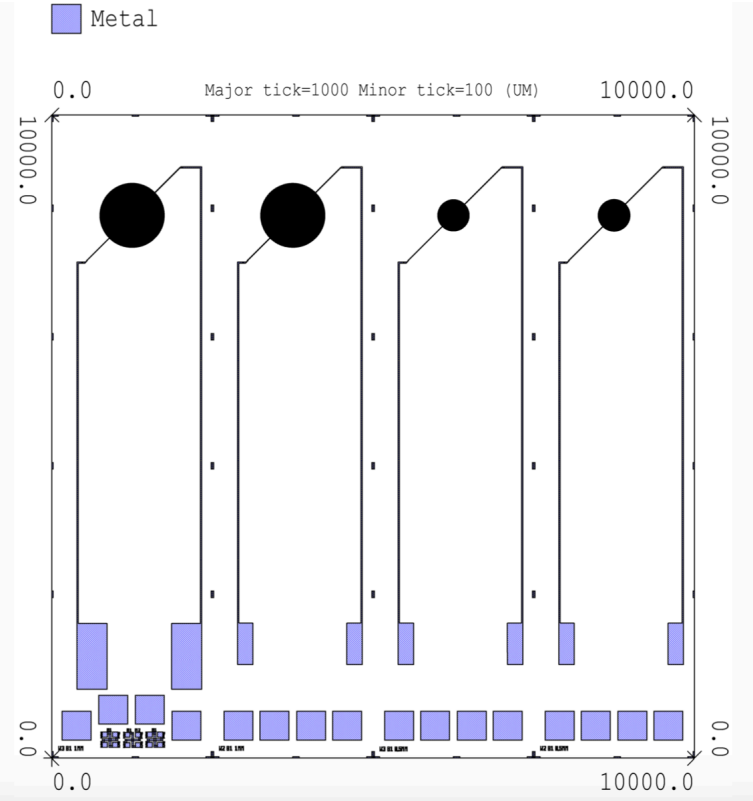

Figure 3.5: Electrodes designed in LabView

In the figure 3.6 shown below, the electrode with Width 3μm, Gap 1μm is shown. Similarly an electrode with Width 2μm, Gap 1μm was also used for measurements.

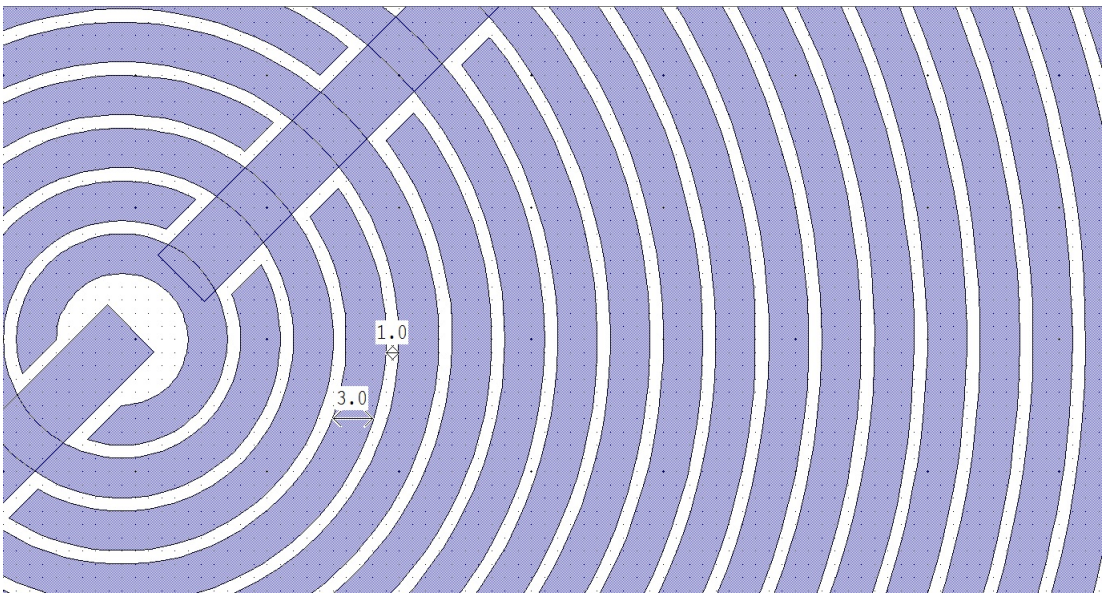

Figure 3.6: Image depicting the Gap and Width of the electrode

In the design above, the electrode with Width 3μm, Gap 1μm is shown. Similarly an electrode with Width 2μm, Gap 1μm was also used for measurements.

3.3. Experimental Setup:

The experimental setup was set in the MEMS lab at EKL. The electrochemical etch process was setup here post the fabrication process. The details regarding the etch process will be briefly discussed in the sections below.

3.3.1. Samples:

The samples used for the electrochemical etching process are the small 10*10 dies, which are diced from the a single fabricated wafer in the earlier step. The dies have 1.7 μm thick p-doped Silicon Carbide layer, which needs to be made porous. Also, the ratio of Si:C varies in the p-doped SiC, there is 50:50 ratio Si:C and a 70:30 ratio Si:C. Alternatively there are samples with SiC from Novellus and are not doped and are processed with a 1.2 μm thickness. And the non doped SiC have no Si:C ratio in particular. These samples are shown below:

3.3.2. Components and materials:

The components and materials used for the experiments are mentioned and discussed below. This experiment consists of an electro-chemical etch set up to make the silicon carbide porous using anodic current and strong acid HF with concentration of 40 percent and 75 percent. The electrochemical etching process is detailed in the experiments section.

- 10*10 samples
- Teflon wires
- Adhesive Glue
- Optical Glue
- Binder machine
- UV-Light
- Current Source
- Hydrofluric Acid
- Platinum electrode
- Plastic beakers

1.10*10 samples : The Silicon Carbide deposited samples as explained above in the samples section were the main specimens for the experiments that were carried out during the etch process for making Porous Silicon carbide.

2.Teflon copper wire : The teflon wire, coloured black and red were used to make electrical connections for an external circuit with the samples and the Current source meter. The choice of a teflon wires was that, they are not easily attacked by the HF.

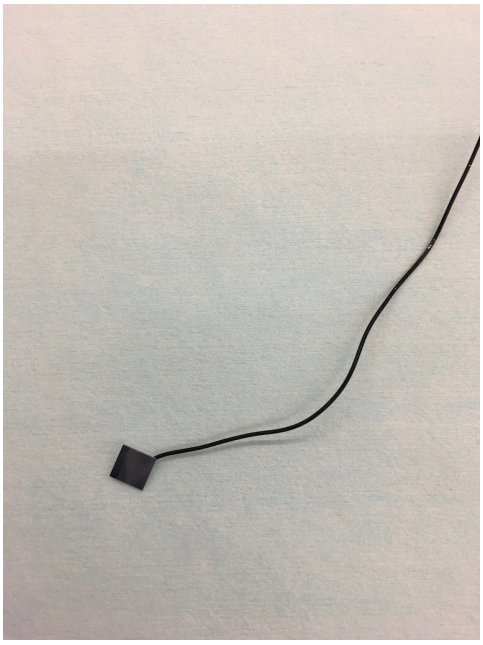

Figure 3.7: 10*10 die glued with a Telfon copper wire

3.Conductive Glue : An Ablestik Conductive glue was used to glue the teflon wires on to the back side samples where Aluminum is used to make a connection for electrical contact.

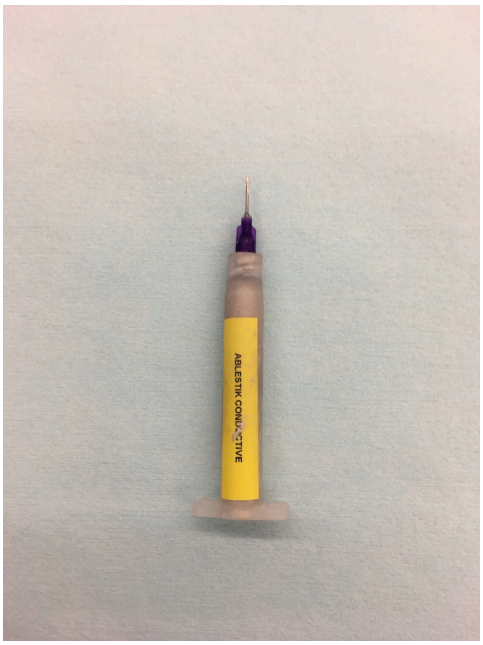

Figure 3.8: Conductive Glue used for making the electrical connection

4.Binder machine : Once the Samples were glued with the conductive Glue, they have to be binded in the binding machine for 2 hours at 120^{o}C. Such that a good contact is made for the external current flow during the electrochemical etching.

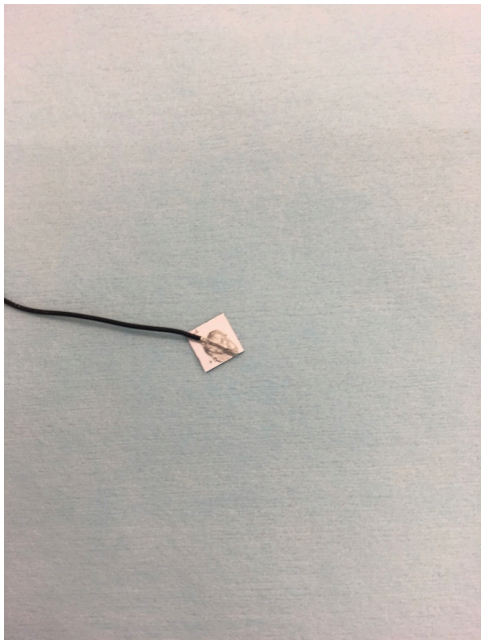

Figure 3.9: The conductive glue after Binding

Figure 3.10: Binding Machine

5.Optical Glue : The optical glue was used to protect the back side of the sample, especially Aluminum, the Conductive Glue from being attacked by HF. Since Aluminum is easily attacked and dissolved by HF, which could lead to the loss electrical contact needed for etching.

Figure 3.11: The optical glue

6.UV- light : Once the samples are coated with the optical glue, it needed to be cured under the UV light for good protection while etching in the HF.

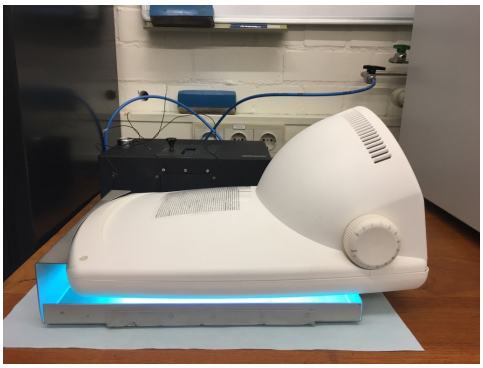

Figure 3.12: Curing the Optical glue with UV light

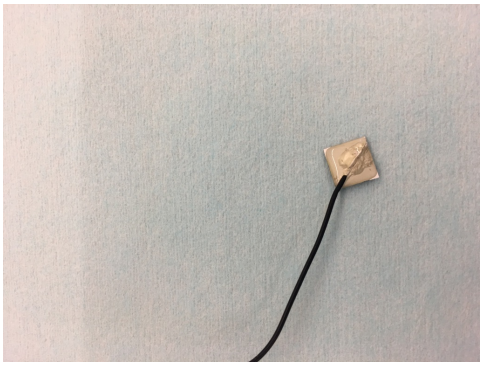

Figure 3.13: Optical glue after curing

7.Current Source : A current source with min to max mA and min to max V is used to supply current

through the external circuit for the etching process.

Figure 3.14: Keithley current source

8.Hydrofluric Acid : A very high concentration of HF is used i.e 70 percent and 40 percent respectively for the etching process. Since SiC is a very robust material is not attacked by any acids or bases, and the only acid that could etch Silicon carbide with high concentration was HF.

Figure 3.15: HF acid 40 percent and 70 percent used for electrochemical etching process

9.Platinum electrode : There is a cathode and an anode during the electrochemical etch process. The cathode used was a Platinum mesh, since Pt is very stable and one the metals other gold which is not attacked by HF. It is not a consumable cathode and hence it can be used several times. Also, Pt is very expensive so it was very mandatory to test if any Pt metal was lost during the process.

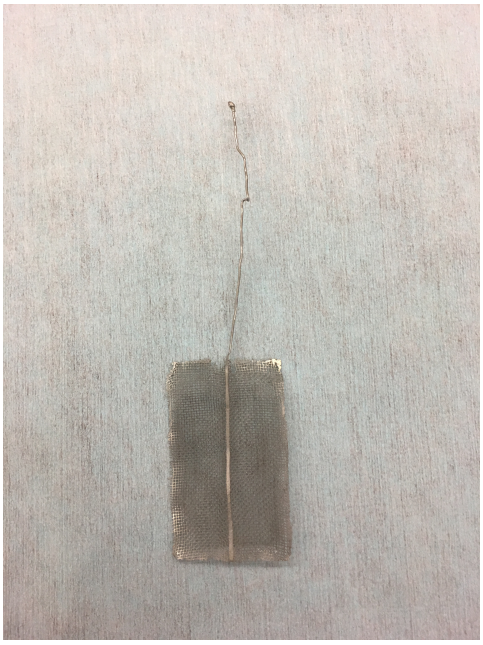

Figure 3.16: Platinum electrode used as cathode

10.Plastic beakers : HF is know to be a very corrosive acid and has the ability to attack a lot of metals and objects that is exposed to it. Glass is one of the material as well which is attacked by HF, hence there was no used of glass ware for the experimental set-up. All plastic beakers and holders were used, since plastic is not easily attacked by HF.

Figure 3.17: Plastic beaker and holder used for etching

3.3.3. Experiments:

The material used was p-doped 1.4-µm-thick SiC thin film from the PVMD lab deposited by plasma-

enhanced chemical vapor deposition (PECVD) on a single-crystalline Si substrate., and undoped 1.2-μm thick SiC deposited by Novellas in the CR 100. Both depositions of SiC are amorphous. A low temperature and deposition rate was employed as it ensures the film was of high quality, especially to avoid generating uneven layer.

In this study, fabrication of a porous layer at the surface of a-SiC thin films by using anodic etching, was performed at a constant current in an aqueous solution with 40 and 75 vol. percent HF. In this experimental setup, the a-SiC anode was placed parallel to the platinum grid cathode; the two electrodes were separated by 2 cm. Prior to anodization, aluminum was evaporated on the back of the sample to create an ohmic contact; this process allowed the a-SiC sample to be used as an electrode. To ensure that only the a-SiC surface was exposed to the electrolyte during anodic etching, the backside and edges of the samples were protected with a optical glue layer, as shown above in the components and materials section. The four edges of the square a-SiC samples were covered by the optical glue leaving 1 × 1 cm2 exposed to the etching solution. Each a-SiC sample was etched at a particular anodic current density from 0.1 to 12 mA/cm2. Because the a-SiC is very resistive, the power source maintained the constant voltage by adjusting the working current from a few volts to more than 10 volts. The etching time for each HF concentration with many samples were noted such that the deepest etch (at an appropriate anodic current density)would be nearly equal to the thickness of few nanometers such that there could be some measurements done with the capacitive based sensor. The surface morphologies of the etched samples were studied with plan-view scanning electron microscopy (SEM).

3.3.4. Electrochemical Etching:

As we known the Silicon Carbide is the most promising material for the fabrication of a new category of sensors and devices, to be used in very hostile environments (height temperature, corrosive ambient, presence of radiation ...). The fabrication of Silicon Carbide sensors requires new processes able to realize micro structures on bulk material or on the silicon carbide surface[53].

A very promising method to create microstructures in SiC is the electrochemical etch in aqueous solution of hydrofluoric acid.This process is explained in detail in the Chapter 4.The formation of deep cavity structures or porous formation as in simple terms in the patterned SiC substrate will be monitored for different wafer having different dopants concentration. The results obtained for the etching rate should go from 0,12 µm /min to up 1.2-1.5 µm /min as reported in the papers. The very promising results are used to create a suspended structures for the fabrication of a piezoresistive SiC pressure sensor for the control of the combustion in a fuel engine[53].

The electrochemistry of the etch process of SiC in HF is based on redox reactions and equations. Where a redox reaction is a reaction which involves a change in oxidation state of one or more elements. When a substance loses its electron, its oxidation state increases, thus it is oxidized. When a substance gains an electron, its oxidation state decreases thus being reduced. For example, for the redox reaction:

$$H2 + F2 \longrightarrow 2HF \tag{3.1}$$

Rewritten as:

- Oxidation : H2 ⟶ 2H+ + 2e-
- Reduction : F2 + 2e- ⟶ 2F-
- Overall Reaction : H2 + F2 ⟶ 2H+ + 2F-

The above equations in electrochemistry is Nernst equations that relates the reduction potential of an electrochemical reaction (half-cell or full cell reaction) to the standard electrode potential, temperature, and activities of the chemical species undergoing reduction and oxidation. It is the most important equation in the field of electrochemistry.

The Nernst equation for an electrochemical half-cell is:

$$E_{red} = E_{red}^{-} - \frac{RT}{zF} lnQ = E_{red}^{-} - \frac{RT}{zF} ln \frac{a_{Red}}{a_{Ox}} \tag{3.2}$$

For a complete electrochemical reaction is :

$$E_{cell} = E_{red}^{-} - \frac{RT}{zF} lnQ_r \tag{3.3}$$

where,

- E_{red} is the half-cell reduction potential at the temperature of interest
- E_{red}^{-} is the standard half-cell reduction potential
- E_{cell} is the cell potential (electromotive force) at the temperature of interest
- E_{cell}^{-} is the standard cell potential
- R is the universal gas constant: R = 8.314472(15) J $K^{-1}\ mol^{-1}$
- T is the temperature in kelvin
- a is the chemical activity for the relevant species, where a_{Red} is the activity of the reduced form and a_{Ox} is the activity of the oxidized form
- F is the Faraday constant, F = $9.64853399(24) * 10^4$ C mol^{-1}
- z is the number of electrons transferred in the cell reaction or half-reaction
- Q_r is the reaction quotient of the cell reaction

4

Results

4.1. Silicon Carbide Etch:

As mentioned in Chapter 3, SiC is deposited above the electrodes. For the capacitive measurements, it requires etching through the SiC to open the capacitor connections of the electrodes.Followed up with an the electrochemical etch process to make the SiC porous.

Dry etching through SiC recipe has not been discussed in any literature, hence this etch through SiC was a trail and error. In the end, it was successfully performed. The recipe and time to etch through SiC, and the machines used is mentioned below:

The chemistry used in etching through SiC is 10 N2/10 B2Cl3/10 Cl2 @ 50W P0.01mTorr. And the equipment used to etch - Alcatel GIR 300. The table below gives

SiC type	Thickness of SiC	Time required for etch
SiC(p-doped)	1.4 μm	55 nm/min
SiC(not doped)	1.2 μm	20 nm/min

Table 4.1: Time taken to etch SiC

4.2. Capacitive Measurements:

The capacitance value changes strongly with the DC voltage applied to the capacitor. Knowing the capacitance value at a specific DC operation point is very important for the correct function of an electronic design.The bare measurements are taken in combination of Vdc with a small Vac. The oscillation voltage is set at 1V and DC bias is 0. And the frequency sweep measurements are taken accordingly.

After fabrication process of the electrodes, and before deposition of the Silicon Carbide as the top layer, the electrodes capacitive measurements were taken. The table below gives the values of the capacitive measurements.

Frequency(Hz)	Capacitance (Cs) pF	Resistance MΩ(Rs)
(W2G1)10k at 0 v_{bias}	3.20956e-011	4.32187e-006
(W2G1020k at 0 v_{bias}	2.16823e-011	4.35907e-006

Table 4.2: Bare capacitance measurements with W2G1 electrode

Frequency(Hz)	Capacitance (Cs) pF	Resistance MΩ(Rs)
(W3G1)10k at 0 v_{bias}	3.27249e-011	3.75381e-006
(W3G1)20k at 0 v_{bias}	2.35546e-011	4.06112e-006
(W3G1)50k at 0 v_{bias}	2.88292e-011	5.87606e-006

Table 4.3: Bare capacitance measurements with W2G1 electrode

* W2G1 = Width 2 Gap 1, W3G1 = Width 3 Gap 1

In the later stage, Silicon Carbide was deposited covering the electrodes and etched through to open the capacitor pads on the die. Followed by which capacitive measurements with SiC layer atop the electrodes was done using the 4-probe measurement machine. The plots of the the measurements is given below.

From the graph's below, the discussion is that we apply an alternating current or AC supply,oscillation voltage is set at 1V. The capacitor will alternately charge and discharge at a rate determined by the frequency of the supply. Then the Capacitance in AC circuits varies with frequency as the capacitor is being constantly charged and discharged. And since, SiC is a highly resistive material, there is an RC parallel circuit obtained.In a system with an applied potential, the current chooses a preferred path (or paths) to travel from one electrode to the other, the path of least impedance.At high frequencies the impedance to current is lower in the capacitor due to its inverse dependence on frequency and therefore smaller than the impedance of a resistor (which is constant at all frequencies). At lower frequencies, the impedance of the capacitor increases and the current begins to flow through the resistor.The characteristics of this system can be determined by the capacitive response at high frequencies and the resistive response at low frequencies.

The capacitive reactance of the capacitor decreases as the frequency across it increases therefore capacitive reactance is inversely proportional to frequency.The opposition to current flow, the electrostatic charge on the plates (its AC capacitance value) remains constant as it becomes easier for the capacitor to fully absorb the change in charge on its plates during each half cycle.Also as the frequency increases the current flowing through the capacitor increases in value because the rate of voltage change across its plates increases. Thus, the above graph of the capacitive measurements show the decrease in capacitance with increase in frequency, except for the data set 4 which doesn't show a normal graph. The reason being so is unknown, but it can be predicted that that data set had some SiC not etched off the capacitor pads and hence the results.

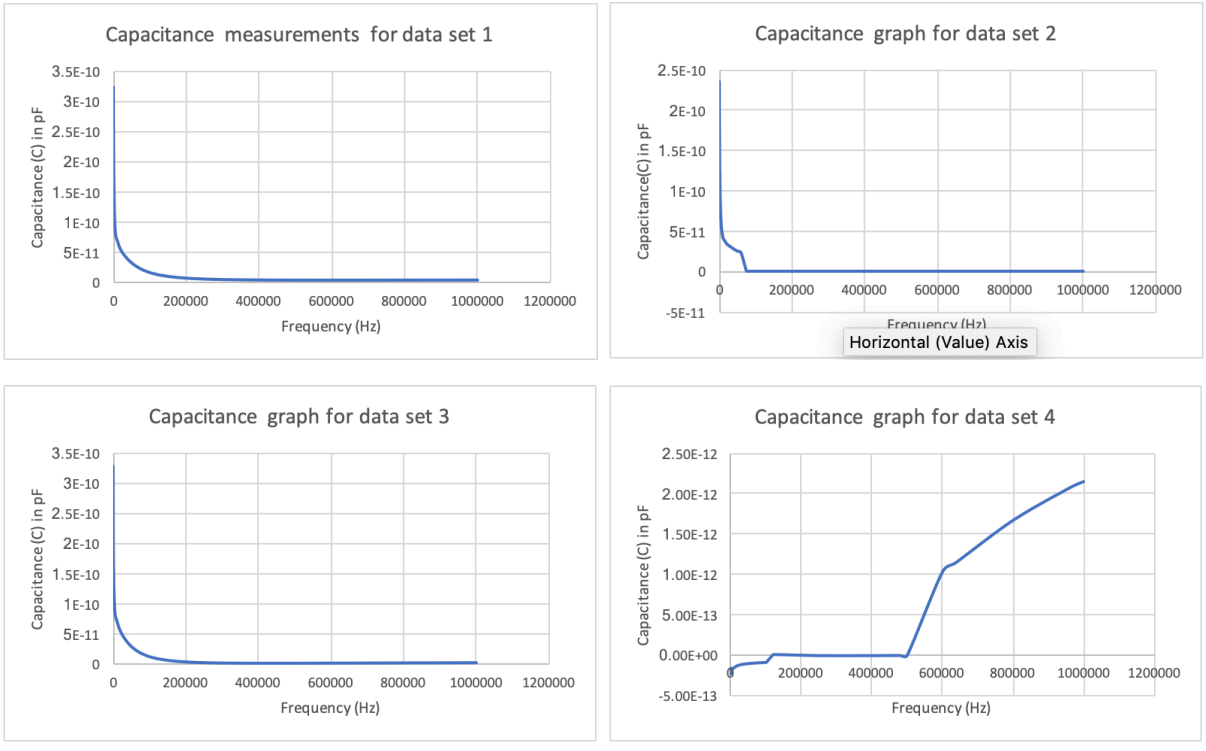

Figure 4.1: Capacitance graph's plotted from data sets of capacitive measurements

Impedance, Z which has the units of Ohms, Ω is the "TOTAL" opposition to current flowing in an AC circuit that contains both Resistance, (the real part) and Reactance (the imaginary part). A purely

resistive impedance will have a phase angle of 0^o while a purely capacitive impedance will have a phase angle of -90^o.

$$ImpedanceZ = V/I \tag{4.1}$$

In the measurement graphs below, the capacitive impedance and theta angle are shown. The impedance(Z) was measured in KΩ rather than MΩ. The values of Z can be referred to in Appendix B.

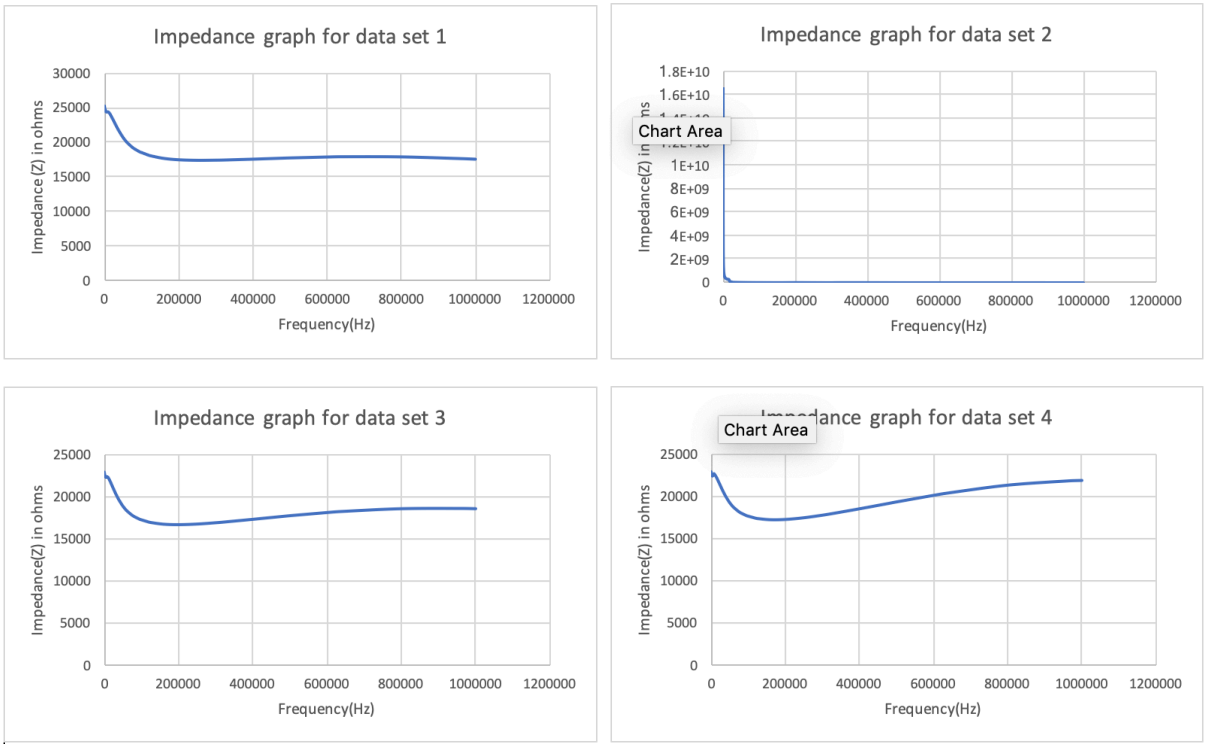

Figure 4.2: Impedance graph plotted from the data sets of capacitive measurements

And from the theta angle measurements, the theta values are no where close to -90^o which is an ideal theta angle for a capacitor. The values can be referred to in Appendix B. And since SiC is highly resistive material, we have a resistor capacitor combination. Also, since the p-doping is very high $1 * 10^{16}(1.0E16)ions/cm^2$ which makes SiC highly conductive which very good for porous formation but not for measurements. Hence the high conductance offered,gives rise to low resistance, thus the theta angles obtained are not good. To improvise the capacitor's behavior and have a good porous formation,along moderate resistance for measurements maybe the semiconducting material SiC could be doped at a lesser concentration. All these measurements were taken before the electrochemical etching of SiC to make it porous. On a further note the chemi-capacitive measurements could not be done as SiC porous formation was not successful.

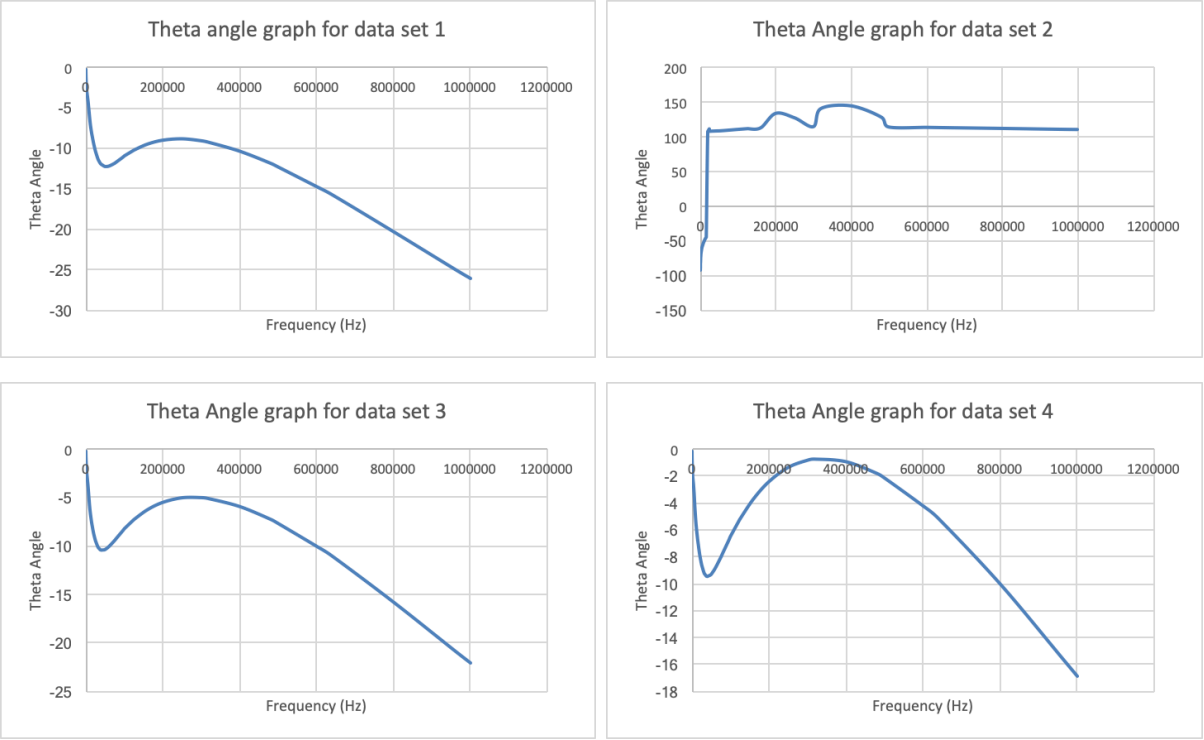

Figure 4.3: Theta Angle plotted from the data sets of capacitive measurements

4.3. Metal Electrodes:

Initially, Aluminum metal was considered as an option for electrodes. As Aluminum is an excellent heat and electricity conductor and in relation to its weight is almost twice as good a conductor as copper. This has made aluminum the most commonly used material in major power transmission lines.

While conducting the electrochemical experiments, with 40 percent and 70 percent HF respectively, the results showed corrosion of the Aluminum metal. Also, Al was used as an back contact for electrical connection to conduct the electrochemical etching for SiC. This also proved that Aluminum is weak and was attacked by HF. The image below show that corrosion of Al.

Figure 4.4: Back contact metal Al corrosion

Further into the experiments, the back contact was re-coated with gold on top of Al. And, then the experiments were carried out and this showed that there was no corrosion with gold and electrical conduction was happening through the metal for the etch process.

Figure 4.5: Gold contact on the backside of the die

In the further process, TiN was considered as electrode material. According to the literature, TiN is not attacked by HF, it just roughens the surface of the TiN. But, while conducting the experiments it showed that TiN was not a robust material towards HF. This attack on TiN was by 70 percent HF. The figure below shows the complete corrosion of TiN. And, 40 percent HF didn't show any corrosion on the metal neither did it etch the SiC.

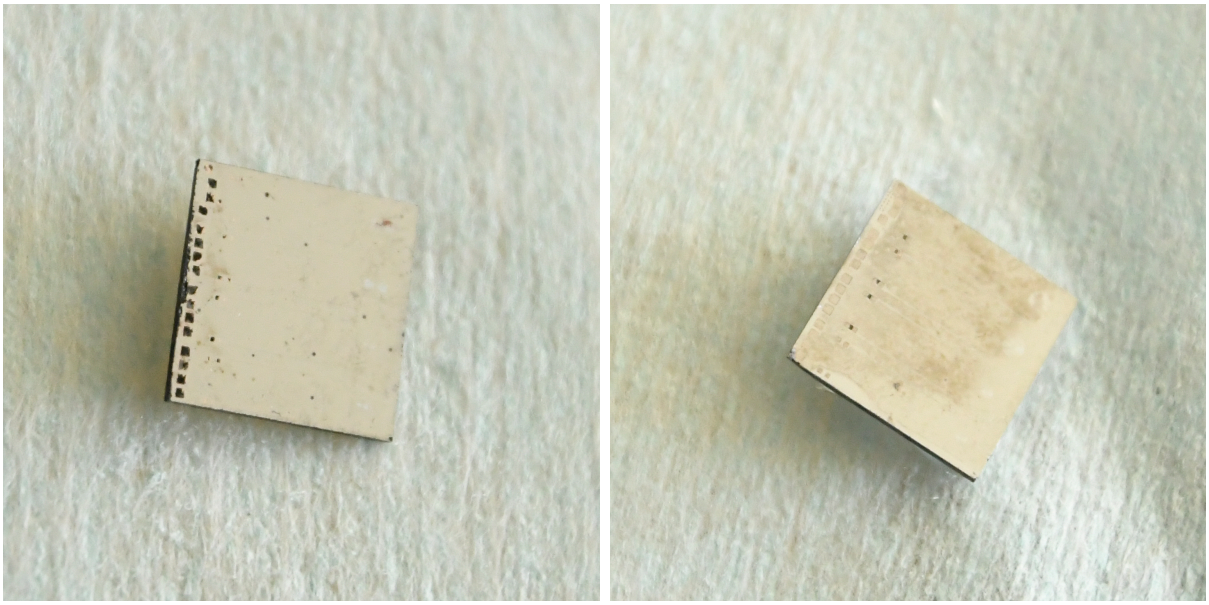

Since, the attack on the TiN electrodes by HF was not expected, and it would affect the capacitance measurements of the device. With no metal electrodes contacts, the device is not suitable for any kind of measurements. Due to this issue with metal electrodes, a suitable metal option has to studied and incorporated for device. Some of the metal options as studied in the literature, is discussed below:

Silver:

- Electrical Properties - High conductivity, Compatible with resistor and dielectric system, Resistivity: $1.59 * 10^{-8} ohm/m$
- Advantage - Least expensive, Good bond strength
- Disadvantage - Low long-term stability disadvantage and the degradation of contacts, Ag can easily move or migrate at temperatures above 300 degrees C

Gold:

- Electrical Properties - High conductivity and reliability, Resistivity: 2.44 $*10^{-8} ohm/m$
- Advantage - High electrical conductivity and reliability
- Disadvantage - Easily diffusing into the substrate (especially silicon) at a relatively low temperature, Very expensive.

Platinum:

- Electrical Properties - Use where extreme resistance to molten solder and to bond strength degradation by solder is required, Resistivity: $11.0 * 10^{-8} ohm/m$
- Advantage - Available wire, flat plate, and tube, Large range of size, Usable at high temperature
- Disadvantage - Most expensive

Palladium-Silver:

- Electrical Properties - Compatible with resistor and dielectric system, Sheet resistance: 0.01–0.04 ohm/sq
- Advantage - Suitable for ultrasonic wire bonding
- Disadvantage - The possibility of silver migration under high humidity

Platinum-Silver:

- Electrical Properties - Alternative to Pd-Ag, Sheet resistance: $0.01–0.04 ohm/sq$
- Disadvantage - Not recommended for hybrid applications

Platinum-Gold:

- Electrical Properties - Compatible with most thick film materials, Sheet resistance: $0.08–0.1 ohm/sq$
- Advantage - Excellent solderability, Suitable for both wire and die bonding
- Disadvantage - High cost, Rather high electrical resistivity

Palladium-Gold:

- Electrical Properties - Similar properties to Pt-Au, Sheet resistance: $0.04–0.10 ohm/sq$
- Advantage - Less expensive than Pt-Au
- Disadvantage - Inferior leach resistance and ageing than Pt-Au

The above listed metals and metal combinations are preferred electrode material, as other metals like Al, Ti, etc., are attacked by HF very easily.

4.4. Electrochemical Reaction:

Electrochemical etching has different modes : Porous formation or electroploshing. Since Silicon Carbide is the most robust material and is not attacked by an acid. The process of porous formation on SiC was tested with electrochemical etching in HF. The process began with 10*10 samples with SiC of 1.7 μm thickness is the anode and a platinum blob is used as the cathode. HF is the electrolyte and the anodic regime for porous formation was performed. The HF concentration used in the first set of experiments is 40 percent.

The results from 40 percent HF etching was no porous formation for low current density of 0.1mA, 0.2mA with a voltage of 10 V and time duration of 1 minute to 10 minutes. The SiC was intact with no reaction.

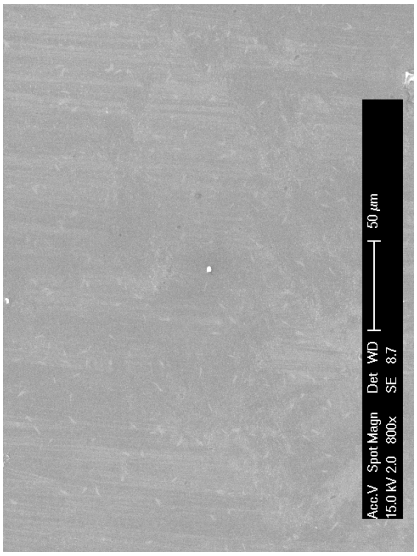

Figure 4.6: SEM image of the of SiC subjected to 40 percent acid. There is only roughness seen.

On the other hand, when the current density was increased to 10mA, 15mA the result was electropolishing of the die. The entire SiC layer on the die was etched. As mentioned above that electropolishing is one of the modes of electrochemical etching. This effect of increase in current density causing electropolishing can be explained in terms of Si with the equations are give below:

(pore formation at low current density)

$$Si + 6HF \longrightarrow H_2SiF_6 + H_2 + 2H^+ + 2e^- \tag{4.2}$$

(electropolishing at high current density)

$$Si + 6HF \longrightarrow H_2SiF_6 + 4H^+ + 4e^- \tag{4.3}$$

The image below shows a die being electropolished.

As, 40 percent HF didn't give any pore formation of SiC. The acid concentration was increased to 70 percent for electrochemical etching. With the increase in the acid concentration and current density of 0.2mA, 0.4mA, 0.6mA and voltage of 10V respectively, the result of the etching was corrosion of the electrodes. There was no sign of pore formation, instead the SiC surface was roughened and the electrodes were subjected to complete corrosion as shown in figure 4.4.

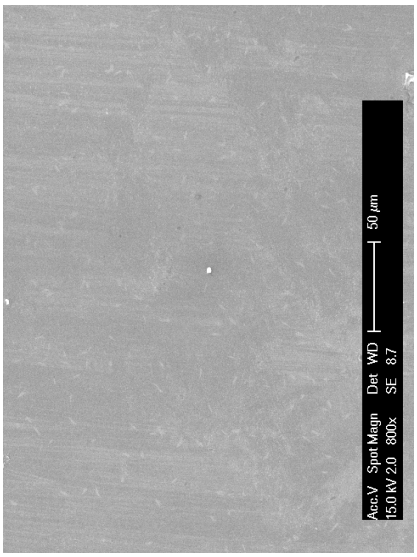

Figure 4.7: SEM image of the of SiC subjected to 70 percent acid. There is only roughness seen.

This process was continued further, to stabilize a current and voltage respectively for the pore formation, but with each die, there was more roughness observed or the electrodes were subjected to intense corrosion. This lead to further research into literature to understand what exactly was the electrochemical reactions that involved in pore formation, which is discussed in the future work.

5

Conclusions and Future work

Every work starts with a goal in mind. This thesis started with a goal to produce a device for humidity and ammonia gas sensor measurements. Various studies and experiments were done to reach the goals of the thesis.The goals were divides into sub-gals and then the study was done. The conclusion in this chapter deals with reviewing the research goals and the directions taken and the what can be at the end concluded form the work.Although, the end results were not as anticipated. It is presented in Section 5.1. The research always opens the doors for new things. It will be discussed in the future work in this chapter in Section 5.2. It will be helpful in taking the research forward and providing directions.

5.1. Conclusions from the work

To discuss about the conclusions, let us first review the research objective and a set of goals at the start of the thesis. Each goal is reviewed in the further and the conclusion derived from goal is discussed. It is also interesting to know how goals are formed but not always it leads to positive achievement of the research objective.

Thesis overview:

From the literature in chapter 2, the study on Silicon carbide and its porous formation has been the center of this thesis. Thus, the obvious option was to conduct experiments on Silicon carbide to test this porosity. Since SiC is a very robust material and is not attacked by any acid, HF with 70 percent concentration was an ideal consideration to make it porous. Although 40 percent HF was also used to test but didn't give any results.

To test the electrochemical etching on the Silicon carbide, the first set of experiments were done. Initially as mentioned in the results chapter, the SiC etching was performed without any electrodes beneath it and using a 40 percent HF. Under the current conditions ranging from 0.1 mA to 10mA with voltage set at 10V and time 10 seconds to 5-6 minutes. This etching gave results such that there was complete electro polishing when current touch 10mA and there was no Etch results(porous formation) below 10mA. It gave two interesting conclusions: a) The 40 percent HF was not too strong for the etching of SiC. b) The higher the current, we could observe electro polishing happening, which is basically removed the SiC layer off the wafer.

Further, the electrochemical etching was carried out with 70 percent HF, a much high concentration, as stated earlier that SiC is very robust to acids. Using this concentration of the acid, gave rise to a lot of uncertainties while conducting the experiments. Firstly, the back contact of the die which had aluminum has the contact for the electrical contact was being attacked despite protecting it with highly viscous optical glue. This issue led to leaking current, since the current never passed through the contact instead passed through the contact and thus reducing the chances of etching and showing a rapid fall in the current. This issue was addressed, and later a gold coating was done on the backside of the die covering the Aluminum. This quite worked well with the HF since Gold cannot be attacked by any acid. Secondly, the electrodes on the front side, we're being attacked by HF and eliminating the chance of capacitive sensing measurements which were to be done in the later stage when SiC is made

porous. Also, at this stage, the etching of SiC to obtain the porosity was still ambiguous since there was roughing of the surface and no porous formation. Roughing is a part of electrochemical process.

It was further studied to find out that the electrochemistry involved to make SiC porous was under light (UV) namely, photoelectrochemical etching. Though, the availability of UV light was ruled out, a simple electrochemistry was used to these experiments. Thus, it became interesting to find out whether it could be achieved.

Overall Conclusions

This thesis concludes three major overall conclusions from the work:

- The electrochemical etching for porous formation gave results in the form of electro polishing or roughening of the surface. The get the porous formation on SiC, the etch process needs a change.
- The TiN electrodes were full-fledged attacked by the HF which destroyed the capacitive sensing of the electrode. This questioned the use of an alternative metal which can be used as electrode material and has equally good dielectric properties.
- The measurement graphs show no good theta angles and impedance values. This is due to the high doping of the SiC, which as explained before is good for porous formation and not for measurements.

5.2. Future Scope

One research always open the doors for the new ones. Thus, it is very important to improve. This thesis gives a lot of scope for the future work. Some of the future work are suggested here.

So far, the electrochemical etching posed some complexities with the porous formation in HF of SiC. Since, SiC is so chemically resistive that only a few techniques are available to etch it. Further literature study showed, the usage of Photoelectrochemical etching (PEC). Photoelectrochemical etching is the process of using ultraviolet light, voltage, and chemicals to etch materials such as silicon carbide which is a robust material to acids.Pure silicon carbide is not a good conductor of electricity so its essential that silicon carbide be doped. If the SiC is n-doped, there are more electrons than holes. Through photoelectrochemical etching, holes are generated with ultraviolet light by breaking some of the bonds in the SiC.Voltage is applied to the sample forcing holes to the surface of the sample to facilitate etching by hydrofluoric acid. Whereas if SiC is p-doped, there are more holes than electrons, which aggravates the hole formation and surfaces them for etching.[54]

SiC nanopores are formed on the substrate surface by PEC. PEC conditions for nanopore formation were: UV light power density of 125 mW/cm2 and a electrical current density of 0.992 mA/cm2 in a HF. Etching is performed for couple of minutes to an hour depending on the concentration of the acid. Nanopore formation is followed by oxidation of the SiC nanopores in a wet oxidation furnace for 4 hours at 1150 degree C which changes the SiC nanopores to SiO2. Finally a chemical etch of the newly formed SiO2 is performed in HF. Photoelectrochemical etching has a more controlled etch rate from low to very high.[54]

- The electrochemical etching can be advanced with usage of UV light to obtain the porous formation of SiC . An in-depth trial and error with the current source values needs to be played with as well to tap in right voltage and current for the etch process.
- The choice of electrodes, has been difficult. Since most of the metals are attacked by HF except for Gold and platinum. Since they have drawbacks, a closer consideration must be done. A detailed chart about Gold and platinum etc. can be read about in the results chapter.

- If,in the long run TiN is considered to be used as the electrode material, it would be best to coat another layer of metal example Al on top of TiN such that when the etch process to make SiC porous is formed, in the time span the HF can attack Al and thus save the TiN underneath by the end of the process.

- Since the capacitive measurements showed not so good results, which is due to the high doping of the SiC material with $1 * 10^16 ions/cm^2$. Which is good porous formation since, it has high conductance but relatively low resistance. And on the other hand, low doping leads to moderate conductance and resistance, but porous formation could be slightly difficult. This balance in obtaining the right doping concentration has to be worked on.

This research did not end up giving the anticipated results at the end but nevertheless I could solve the loop holes which will lead to a better execution of this research in the future. In the words of Sir Einstein, I would like to quote:

"I have not failed. I've just found 10,000 ways that won't work"

A

Ammonia sensor

Flow chart

Version 1
22 June 2018
Tom Scholtes

Process number: P3366
Process engineer: Samyuktha Jagarlamudi
Mentor: Mario
Start: 1st July

Contamination:
Labs: SiC Solar cell lab

EKL(Else Kooi Laboratory)
DELFT UNIVERSITY OF TECHNOLOGY
Address : Feldmannweg 17, 2628 CT Delft, The
P.O. Box: 5053, 2600 GB Delft, The Netherlands
Phone : +31 - (0)15 - 2783868
Fax : +31 - (0)15 - 2622163
Website : http://ekl.tudelft.nl/EKL/Home.php

Detailed information about possible contamination:

Place/Clean Rooms used in process:

- **Write the sequence of used labs from start to finish.**
- **Which (Non-standard) materials or process steps**
- **Process step number**
- **What kind of process or machine was used?**
- **The other materials or wafers that contain non-green metals that are also processed in this machine**

Example

Lab/ Clean Room	Non-standard materials	Process step	Machine-process	Other materials used in machine
CR10000	SiC	PECVD deposition		Other green metals like gold, chromium etc..

If there are custom steps in a standard process or possible cross contamination materials are used: Write down the

- **Step number**
- **Material**
- **Machine/tool where the process is done**
- **Pre and past process step numbers that are used to prevent cross contamination.**

Example

Step number	Material	Machine/Tool/lab	Process steps to prevent cross contamination
-	-	-	-

GENERAL RULES

CLEANROOM BEHAVIOUR

Always follow the "**Security and Behaviour**" rules when working in the EKL laboratories.

Always handle wafers with care during processing. Use cleanroom gloves and work as clean as possible!!

Use cleanroom gloves when working with vacuum equipment. Do not touch the inside or carriers with bare hands.

Always check equipment and process conditions before starting a process. Do **NOT** make unauthorized changes!

Directly notify the responsible staff member(s) when there are problems with equipment (like malfunction or contamination). Put the system down in the Phoenix reservation system, and turn the equipment status sign from UP or Usable to DOWN.

DO NOT TRY TO REPAIR OR CLEAN EQUIPMENT YOURSELF, and **NEVER** try to refresh a contaminated etch or cleaning bath! Only authorized staff members are allowed to do this.

PCC RULES

All substrates, layers and chemicals which are not CMOS compatible are considered to be "**NON-STANDARD**" materials, and may be contaminating.

The use of "non-standard" materials for processing in the class100 and SAL cleanroom must **ALWAYS BE EVALUATED AND APPROVED** by your mentor and in agreement with the PCC document.
Wafers that are contaminated may **NEVER** be processed in any of the equipment without permission of the Equipment owner Special precautions may have to be taken, like the use of a special substrate holder or container.

Check the PCC "Rules & Instructions" - available on the "EKL intranet webpage" - for more details.

CLASS 100 RULES

CLEANING OF WAFERS

After several hours (4 hours max) of storage wafers must always be cleaned before performing a **COATING, FURNACE, EPITAXY** or **DEPOSITION** step.

Use the correct cleaning procedure:

- Tepla stripper ⇨ for removal of implanted or plasma etched photoresist
- Acetone ⇨ for removal of photoresist that is not implanted or plasma etched
- HNO_3 99% (Si) ⇨ for IC compatible wafers which do not need a HNO_3 69.5% step
- HNO_3 99% (Al) ⇨ for wafers which are or have been in contact with one of the following metals: like Al, Al(1%Si), Ge, Ti, Zr
- HNO_3 99% (Si) + HNO3 69.5% (Si) ⇨ for all other IC compatible wafers

Note:
- The above described cleaning procedures are only valid for IC compatible wafers with "standard" materials on them. **In all other situations follow the PCC rules (Previously to be discussed with the mentor).**
- Wafers do not have to be cleaned **after** a furnace, epitaxy or deposition step if the next process step will be performed immediately, unless the wafers are covered with particles.

FURNACE RESTRICTIONS

Wafers that are covered with photoresist or a metal layer may **NEVER** be processed in any of the furnaces. This also applies for wafers from which a metal layer has been removed by etching. Only alloying in tube C4 is allowed for wafers with an aluminium layer.

MEASUREMENTS

Always perform all the measurement and inspection steps, and **write down the results in your journal and in the result tables that can be found at some of the equipment!!** The results are used to check the condition of the processes and/or equipment.

It is possible to use the following Class 100 equipment to measure directly onto your (IC compatible) process wafers:

- The Leitz MPV-SP, the WOOLLAM and the SAGAX. These systems are used for thickness measurements of transparent layers. The measurements are non-destructive and without contact to the wafer surface.
- The Dektak 8 surface profilometer. This system is used for step height measurements. In this case a needle will physically scan over the wafer surface (contact measurement), which can be destructive for structures.
- The XL50 SEM. It can be used for inspection of your wafers and for width, depth or thickness measurements.

Note: **After certain measurements cleaning of your wafers may be required for further processing.**

An extra wafer must be processed when other measurement methods will be used (like sheet resistance and junction depth measurements). These wafers cannot be used for further processing.

STARTING MATERIAL

Use 10 **SINGLE SIDE** polished with preprocessing on front and backside from outside EKL with the following specifications:

Type:	p/B (p-type, boron)
Orientation:	<100>
Resistivity:	2-5 Ωcm
Thickness:	525 ± 15 µm
Diameter:	100 mm
Number of wafer:	10 (10 with waveguide cores).

Mask set: EC2091
Mask box: 475
Die size: 10x10mm

1. COATING AND BAKING.

Nov 2008

Use the coater station of the EVG120 system to coat the wafers with photoresist. The process consists of:

- a treatment with HMDS (hexamethyldisilazane) vapor, with nitrogen as a carrier gas
- spin coating of Shipley AZ-ECI3027 positive resist, dispensed by a pump
- a soft bake at 95 °C for 90 seconds
- an automatic edge bead removal with a solvent

Always check the relative humidity (48 ± 2 %) in the room before coating, and follow the instructions for this equipment.

Use program "1 **Co -Zero layer.**

2. ALIGNMENT AND EXPOSURE

- **May 2011**

Processing will be performed on the ASML PAS5500/80 automatic wafer stepper.
Follow the operating instructions from the manual when using this machine.

Expose masks **COMURK** and with job "**COMURK0.0**" and the correct exposure energy 150mJ
This results in alignment markers for the stepper and contact aligner for wafers which will not get an EPI layer.

3. DEVELOPING:

- **Apr 2008**

Use the developer station of the EVG120 system to develop the wafers. The process consists of:

- a post-exposure bake at 115 °C for 90 seconds
- developing with Shipley MF322 with a single puddle process
- a hard bake at 100 °C for 90 seconds

Always follow the instructions for this equipment.

Use program " 1 **Dev - SP**".

4. INSPECTION:

- **Feb 1996**

Visually inspect the wafers through a microscope. No resist residues are allowed

5. PLASMA ETCHING: PM (primary alignment markers) into Silicon

• **Feb 1999**

Use the Trikon Ωmega 201 plasma etcher.
Follow the operating instructions from the manual when using this machine.
It is **not** allowed to change the process conditions and times from the etch recipe!

Use sequence **URK_NPD** (with a platen temperature of **20 °C**) to etch 120nnm deep into the Si.

Process conditions from chamber recipe URK_NPD:						
Step	Gasses & flows	Pressure	Platen RF	ICP RF	Platen temp.	Etch time
2. bulk etch	O2/SF6= 20/2O sccm	50 mTorr	15 W	500 W	10 °C	1m30sec

6. LAYER STRIPPING: Photoresist

• **Feb 1999**

Strip resist — Use the Tepla Plasma 300 system to remove the photoresist in an oxygen plasma. Follow the instructions specified for the Tepla stripper, and use the quartz carrier. Use **program 1**: 1000 watts power and automatic endpoint detection + 2 min. over etching.

7. CLEANING AND HF DIP: HNO_3

• **Sept 1998**

Clean — 10 minutes in fuming nitric acid at ambient temperature. This will dissolve organic materials. Use wet bench "HNO_3 99% (Si)" and the carrier with the red dot.

Rinse — Rinse in the Quick Dump Rinser with the standard program until the resistivity is 5 MΩ.

Clean — 10 minutes in concentrated nitric acid at 110 °C. This will dissolve metal particles. Use wet bench "HNO_3 69,5% 110C (Si)" and the carrier with the red dot.

Rinse — Rinse in the Quick Dump Rinser with the standard program until the resistivity is 5 MΩ.

Native oxide removal — Use wetbench "0.55% HF/IPA" and the carrier with the yellow + black dots. Etchtime: **4 minutes** at ambient temperature. The wafer must be **hydrophobic**.

QDR — Rinse in the Quick Dump Rinser with the standard program until the resistivity is 5 MΩ.

Dry — Use the Avenger Ultra pure-6 "rinser/dryer" with the standard program, and the white carrier with a red dot.

NOTE: Immediately after drying, the oxidation must be performed.

8. WET OXIDATION (300A)

• **Jan 1995**

Furnace no: C1 Program name: 300A Total time: 70 min

PROCESS	TEMPERATURE (in °C)	GASSES & FLOWS (in liter/min)	TIME (in minutes)	REMARKS
boat in	600	nitrogen: 6.0	5	
heat up	+10 °C/min	nitrogen: 3.0 oxygen: 0.3	25	
stabilize	850	nitrogen: 3.0 oxygen: 0.3	5	
oxidation	850	oxygen: 2.25 hydrogen: 3.85	20	
cool down	-5 °C/min	nitrogen: 3.0	10	
boat out	-5 °C/min	nitrogen: 3.0	5	

9. MEASUREMENT: Oxide thickness

- **Oct 1996 2002**

Use the WOOLLAM measurement system for layer thickness measurements.
Follow the operating instructions from the manual when using this equipment.

⇨ Program: oxide

10. BORON IMPLANTATION: Back side

- **Jan 1995**

Ion B^+
Energy 40 keV
Dose 1×10^{16} (1.0E16) ions/cm^2

Remarks The angle of implant is standard 7 deg.
The flat side of the wafer must be turned 22 deg north east.

11. CLEANING: HNO_3 99% and 69.5%

- **Sept 1998**

Clean 10 minutes in fuming nitric acid at ambient temperature. This will dissolve organic materials.
Use wet bench "HNO_3 99% (Si)" and the carrier with the red dot.
Rinse Rinse in the Quick Dump Rinser with the standard program until the resistivity is 5 MΩ.
Clean 10 minutes in concentrated nitric acid at 110 °C. This will dissolve metal particles.
Use wet bench "HNO_3 69,5% 110C (Si)" and the carrier with the red dot.
Rinse Rinse in the Quick Dump Rinser with the standard program until the resistivity is 5 MΩ.

Dry Use the Avenger Ultra pure-6 "rinser/dryer" with the standard program, and the white carrier with a red dot.

12. ANNEALING IN ARGON GAS

- **Jan 1995**

Furnace tube: C2 **Program name: ANNEALN1** **Total time: 165 min**

PROCESS	TEMPERATURE (in °C)	GASSES & FLOWS (in liter/min)	TIME (in minutes)	REMARKS
boat in	600	argon: 6.0	5	Argon shower
stabilize	600	argon: 6.0	10	
anneal	600	argon: 6 .0	20	
heat up	+10 □C/min	argon: 3.0	40	
stabilize	1000	argon: 3.0	10	
anneal	1000	argon: 3.0	35	
cool down	-5 □C/min	argon: 3.0	40	
boat out	800	argon: 3.0	5	Argon shower

Note:
- **ALWAYS perform this step BEFORE metallization!**
- **Each process wafer must be placed between two dummy wafers!**

13. OXIDE STRIP BHF:

- **Apr 2008**

Etching Use wet bench "BHF at ambient temperature, and the carrier with the blue dot.
The bath contains standard 0.55% HF solution (Merck, VLSI selectipur).
Etch time Until hydrophobic + 20seces.
QDR Rinse in the Quick Dump Rinser with the standard program until the resistivity is 5 MΩ.
Drying Use the Avenge r Ultra pure-6 "rinser/dryer" with the standard program, and the orange carrier with a red dot.

14. CLEANING: HNO_3 99% and 69.5%

• **Sept 1998**

Clean	10 minutes in fuming nitric acid at ambient temperature. This will dissolve organic materials. Use wet bench "HNO_3 99% (Si)" and the carrier with the red dot.
Rinse	Rinse in the Quick Dump Rinser with the standard program until the resistivity is 5 MΩ.
Clean	10 minutes in concentrated nitric acid at 110 °C. This will dissolve metal particles. Use wet bench "HNO_3 69,5% 110C (Si)" and the carrier with the red dot.
Rinse	Rinse in the Quick Dump Rinser with the standard program until the resistivity is 5 MΩ.
Dry	Use the Avenger Ultra pure-6 "rinser/dryer" with the standard program, and the white carrier with a red dot.
Remove native oxide	Use 4 minutes 0.55% HF at ambient temperature. The wafer must be **hydrophobic**. Use wet bench "0.55% HF" and the carrier with the black dots.
Rinse	Rinse in the Quick Dump Rinser with the standard program until the resistivity is 5 MΩ.
Dry	Use the Avenger Ultra pure-6 "rinser/dryer" with the standard program, and the white carrier with a black dot.

Note **The next step must be performed immediately after drying.**

15. FIRST METALLIXATION: Sputtering of 1000nm Al/Si: Backside

• **Jan 2000**

Use the TRIKON SIGMA sputter coater for the deposition of an aluminium metal layer on the wafers.
The target must exist of 99% Al and 1% Si, and deposition must be done at 350 °C with an Ar flow of 100 sccm.
Follow the operating instructions from the manual when using this machine.

Use recipe **675nm Al @ 350C** to sputter a 675nm thick layer.

Visual inspection: the metal layer must look shiny.

16. TITANIUM-NITRIDE SPUTTERING: 350nm TiN @ 350°C

• **Jan 2000**

Use the TRIKON SIGMA 204 sputter coater for the deposition of a Titanium and Titanium-nitride on the wafers.
The target must exist Ti and deposition must be done at 350 °C.
Follow the operating instructions from the manual when using this machine.

Use recipe **TiN 350nm_350C** to obtain a 350nm thick TiN stacked layer.

Note: Use dummy wafer in between process wafers to clean the target.
Use the same temperature in this in between recipe as the process recipe.

Visual inspection: the metal layer must look.

17. COATING AND BAKING

• **Apr 2008**

Use the coater station of the EVG120 system to coat the wafers with photoresist. The process consists of:
- a treatment with HMDS (hexamethyldisilazane) vapor, with nitrogen as a carrier gas
- spin coating of Shipley SPR3012 positive resist, dispensed by a pump
- a soft bake at 95 °C for 90 seconds
- an automatic edge bead removal with a solvent

Always check the relative humidity (48 ± 2 %) in the room before coating, and follow the instructions for this equipment.

Use program "1 **Co - 3012-1.4µm**".

18. ALIGNMENT AND EXPOSURE: Metal mask

• **Sept 1998**

Processing will be performed on the ASML PAS5500/80 automatic wafer stepper.
Follow the operating instructions from the manual when using this machine.

Use **mask: Metal**, **Box = 475 Job: 10*10_4img, Layer 4, ID = 2*2** and **Exposure energy = 150mJ/cm2**

19. DEVELOPING

• **Apr 2008**

Use the developer station of the EVG120 system to develop the wafers. The process consists of:
- a post-exposure bake at 115 °C for 90 seconds
- developing with Shipley MF322 with a double puddle process
- a hard bake at 100 °C for 90 seconds

Always follow the instructions for this equipment.

Use program "1 **Dev – SP**

20. INSPECTION: Line width and overlay

• **Feb 1996**

Visually inspect the wafers through a microscope. No resist residues are allowed.

21. PLASMA ETCH TiN: 1st metal (350 nm sputtered at 350°C)

• **Aug 2002**

Use the Trikon Ωmega 201 plasma etcher.
Follow the operating instructions from the manual when using this machine.
The process conditions of the etch and passivation program may not be changed !

Use sequence **tinti_2** and set the platen temperature to **25 °C** to etch the TiN layer (sputtered at **350°C**).

Metal etch conditions of chamber recipe ???????:						
Step	Gasses & flows	Pressure	Platen RF	ICP RF	Platen temp.	Etch time
1. breakthrough	HBr/Cl_2 = 40/30 sccm	5 mTorr	50 W	500 W	25 °C	endpoint
2. bulk etch	HBr/Cl_2 = 40/30 sccm	5 mTorr	40 W	500 W	25 °C	endpoint
3. overetch	HBr/Cl_2 = 30/15 sccm	5 mTorr	40 W	500 W	25 °C	50% of bulk

INSPECTION: No TiN residues or under etching are allowed.

22. LAYER STRIPPING: Photoresist

• Feb 1999

Strip resist Use the Tepla Plasma 300 system to remove the photoresist in an oxygen plasma.
Follow the instructions specified for the Tepla stripper, and use the quartz carrier.
Use **program 1**: 1000 watts power and automatic endpoint detection + 2 min. over etching.

23. CLEANING PROCEDURE: HNO_3 99% metal

• Jan 1995

Cleaning 10 minutes in fuming nitric acid (Merck: HNO_3 100% selectipur) at ambient temperature.
Use wet bench "HNO_3 (100%) **metaal**" and the carrier with the yellow and red dots.
QDR Rinse in the Quick Dump Rinser with the standard program until the resistivity is 5 MΩ.
Drying Use the Avenger Ultra pure-6 "rinser/dryer" with the standard program, and the white carrier with a black dot.

NOTE: No 65% HNO_3 cleaning step!

24. PECVD DEPOSITION: P-doped Silicon Carbide.

• Jan 1995

Use CR10000 PECVD reactor.
Follow the operating instructions from the manual when using this machine.
It is **not** allowed to change the process conditions and time from the deposition recipe!

Use macro recipe to deposit a 1.7 μm thick SiC layer.

Process conditions from recipe DI04SiC100:					
Gasses & flows	Pressure	HF power	LF power	Temperature	Time
SiH_4/CH_4 = 100/3000 sccm	2.0 Torr	250 W	750 W	400 °C	65.0 $^{sec}/_{station}$

Note:
- The CH_4 gas flow is being controlled with a mass flow controller that is calibrated for NH_3. The setpoint in the process recipe on the machine to get a CH_4 flow of 3000 sccm is equivalent to 4110 sccm NH_3.
- The deposition time is subject to minor changes, in order to obtain the correct film thickness.

POSIBLE CONTAMINATION OF WAFERS

B

Capacitive and resistive measurements set 1 with SiC layer above the electrodes with full sweep

BEGIN_HEADER																	
	ICCAP_INPUTS																
!	<Name>	<Mode>	<+	Node>	<-	Node>	<Unit>	<Compliance>	<Sweep-type>	<Ratio>	<Offset>	<Master	Sweep>				
	Cval	V	DEFAULT	GROUND	DEFAULT	0	SYNC	1	0	Freq							
!	<Name>	<Mode>	<+	Node>	<-	Node>	<Unit>	<Compliance>	<Sweep-type>	<Ratio>	<Offset>	<Master	Sweep>				
	Gval	V	DEFAULT	GROUND	DEFAULT	0	SYNC	1	0	Freq							
!	<Name>	<Mode>	<+	Node>	<-	Node>	<Unit>	<Compliance>	<Sweep-type>	<Sweep	Order>	<Start>	<Stop>	<#	of	Points>	
	Freq	V	DEFAULT	GROUND	DEFAULT	0	LIN	1	0	0	71	0					
	ICCAP_OUTPUTS																
END_HEADER																	
BEGIN_DB																	
	Freq	Cval	Gval		Freq	Cval	Gval		Freq	Cval	Gval		Freq	Cval	Gval		
	100	8,62E-12	2,09E+10		500	2,63E-10	25075,9		10000	7,04E-11	24522,6		125000	1,24E-11	18341,2		
	100	8,62E-12	2,09E+10		600	2,46E-10	25043,8		12000	6,71E-11	24490,3		160000	9,19E-12	17928,1		
	100	8,62E-12	2,09E+10		750	2,27E-10	25002,5		15000	6,14E-11	24315,9		200000	7,06E-12	17703,7		
	100	8,62E-12	2,09E+10		800	2,21E-10	24990,1		16000	5,96E-11	24240,1		250000	5,56E-12	17619,9		
	100	8,62E-12	2,09E+10		1000	2,03E-10	24936,3		20000	5,42E-11	23900		300000	4,76E-12	17649,9		
	100	8,62E-12	2,09E+10		1200	1,90E-10	24893,3		24000	5,01E-11	23543,4		320000	4,55E-12	17678,8		
	100	8,62E-12	2,09E+10		1250	1,86E-10	24883,6		25000	4,92E-11	23449,1		400000	4,04E-12	17865		
	100	8,62E-12	2,09E+10		1500	1,71E-10	24827,9		30000	4,50E-11	22967,4		480000	3,82E-12	18103,8		
	100	8,62E-12	2,09E+10		1875	1,53E-10	24753,4		32000	4,36E-11	22775,9		500000	3,80E-12	18168,5		
	100	8,62E-12	2,09E+10		2000	1,48E-10	24732,2		37500	3,97E-11	22256,1		600000	3,75E-12	18489,6		
	100	2,36E-10	25184,4		2400	1,32E-10	24663,7		40000	3,80E-11	22030,8		640000	3,74E-12	18616,3		
	120	2,77E-10	25213,7		2500	1,29E-10	24647,2		48000	3,34E-11	21346,5		800000	3,84E-12	19079,3		
	150	3,10E-10	25217,4		3000	1,16E-10	24572,6		50000	3,24E-11	21186		960000	3,95E-12	19463,2		
	200	3,22E-10	25202		3750	1,01E-10	24485		60000	2,78E-11	20488,4		1,00E+06	3,97E-12	19548		
	250	3,20E-10	25181,4		4000	9,73E-11	24466,6		75000	2,24E-11	19698						
	300	3,09E-10	25158,4		5000	8,66E-11	24427,5		80000	2,09E-11	19490,4						
	375	2,94E-10	25123,2		6000	7,98E-11	24429,8		96000	1,71E-11	18951,4						
	400	2,85E-10	25113,1		7500	7,48E-11	24483,1		100000	1,62E-11	18869,2						
	480	2,68E-10	25081,3		8000	7,36E-11	24507,6		120000	1,31E-11	18424,7						

Capacitive and resistive measurements set 2 with SiC layer above the electrodes with full sweep

BEGIN_HEADER																	
	ICCAP_INPUTS																
!	<Name>	<Mode>	<+	Node>	<-	Node>	<Unit>	<Compliance>	<Sweep-type>	<Ratio>	<Offset>	<Master	Sweep>				
	Cval	V	DEFAULT	GROUND	DEFAULT	0	SYNC	1	0	Freq							
!	<Name>	<Mode>	<+	Node>	<-	Node>	<Unit>	<Compliance>	<Sweep-type>	<Ratio>	<Offset>	<Master	Sweep>				
	Gval	V	DEFAULT	GROUND	DEFAULT	0	SYNC	1	0	Freq							
!	<Name>	<Mode>	<+	Node>	<-	Node>	<Unit>	<Compliance>	<Sweep-type>	<Sweep	Order>	<Start>	<Stop>	<#	of	Points>	
	Freq	V	DEFAULT	GROUND	DEFAULT	0	LIN	1	0	0	71	0					
	ICCAP_OUTPUTS																
END_HEADER																	
BEGIN_DB																	
	Freq	Cval	Gval		Freq	Cval	Gval		Freq	Cval	Gval		Freq	Cval	Gval		
	100	8,62E-12	2,09E+10		500	1,92E-10	54493		10000	4,18E-11	54425,8		125000	4,51E-15	2,93E+08		
	100	8,62E-12	2,09E+10		600	1,83E-10	54369		12000	3,97E-11	54832,1		160000	5,87E-15	3,97E+08		
	100	8,62E-12	2,09E+10		750	1,72E-10	54242		15000	3,79E-11	54576,9		200000	7,10E-15	6,92E+08		
	100	8,62E-12	2,09E+10		800	1,69E-10	54212		16000	3,71E-11	54463,1		250000	8,66E-15	3,09E+09		
	100	8,62E-12	2,09E+10		1000	1,43E-10	54050		20000	3,42E-11	54487,9		300000	1,00E-14	-1,42E+09		
	100	8,62E-12	2,09E+10		1200	1,36E-10	53924		24000	3,25E-11	53722,8		320000	1,04E-14	-8,39E+08		
	100	8,62E-12	2,09E+10		1250	1,33E-10	53891		25000	3,23E-11	53538,3		400000	1,20E-14	-6,61E+08		
	100	8,62E-12	2,09E+10		1500	1,25E-10	53635		30000	3,07E-11	52512,4		480000	1,30E-14	-1,49E+09		
	100	8,62E-12	2,09E+10		1875	1,16E-10	53323		32000	3,01E-11	52037,2		500000	1,45E-14	8,28E+08		
	100	8,62E-12	2,09E+10		2000	1,08E-10	53304		37500	2,83E-11	50820,1		600000	1,55E-14	2,20E+08		
	100	1,18E-10	55421,5		2400	9,68E-11	53010		40000	2,75E-11	50253,8		640000	1,57E-14	1,48E+08		
	120	1,75E-10	55446,7		2500	9,45E-11	52955		48000	2,54E-11	48506,4		800000	1,59E-14	7,34E+07		
	150	2,18E-10	55394,6		3000	8,50E-11	52657		50000	2,50E-11	48110,5		960000	1,58E-14	4,49E+07		
	200	2,35E-10	55256,2		3750	7,36E-11	52289		60000	2,29E-11	46196		1,00E+06	1,58E-14	4,03E+07		
	250	2,34E-10	55080,1		4000	7,06E-11	52239		75000	4,28E-15	2,45E+08						
	300	2,25E-10	54949,5		5000	6,12E-11	52186		80000	3,86E-15	2,46E+08						
	375	2,11E-10	54722,4		6000	5,46E-11	52388		96000	3,87E-15	2,55E+08						
	400	2,05E-10	54675,8		7500	4,88E-11	53099		100000	3,79E-15	2,61E+08						
	480	1,94E-10	54501,1		8000	4,74E-11	53376		120000	4,37E-15	2,96E+08						

Capacitive and resistive measurements set 3 with SiC layer above the electrodes with full sweep

BEGIN_HEADER																
	ICCAP_INPUTS															
!	<Name>	<Mode>	<+	Node>	<-	Node>	<Unit>	<Compliance>	<Sweep-type>	<Ratio>	<Offset>	<Master	Sweep>			
	Cval	V	DEFAULT	GROUND	DEFAULT	0	SYNC	1	0	Freq						
!	<Name>	<Mode>	<+	Node>	<-	Node>	<Unit>	<Compliance>	<Sweep-type>	<Ratio>	<Offset>	<Master	Sweep>			
	Gval	V	DEFAULT	GROUND	DEFAULT	0	SYNC	1	0	Freq						
!	<Name>	<Mode>	<+	Node>	<-	Node>	<Unit>	<Compliance>	<Sweep-type>	<Sweep	Order>	<Start>	<Stop>	<#	of	Points>
	Freq	V	DEFAULT	GROUND	DEFAULT	0	LIN	1	0	0	71	0				
	ICCAP_OUTPUTS															
END_HEADER																
BEGIN_DB																
	Freq	Cval	Gval		Freq	Cval	Gval		Freq	Cval	Gval		Freq	Cval	Gval	
	100	8,62E-12	2,09E+10		500	2,37E-10	22698,6		10000	7,39E-11	22352,5		125000	9,53E-12	16986,9	
	100	8,62E-12	2,09E+10		600	2,21E-10	22676,1		12000	6,95E-11	22250,4		160000	6,49E-12	16745,2	
	100	8,62E-12	2,09E+10		750	2,05E-10	22649,2		15000	6,36E-11	22036,8		200000	4,58E-12	16668,1	
	100	8,62E-12	2,09E+10		800	2,00E-10	22641,6		16000	6,17E-11	21950,2		250000	3,33E-12	16728,1	
	100	8,62E-12	2,09E+10		1000	1,84E-10	22608,3		20000	5,58E-11	21591,5		300000	2,74E-12	16883,9	
	100	8,62E-12	2,09E+10		1200	1,72E-10	22584,4		24000	5,09E-11	21224,8		320000	2,62E-12	16960	
	100	8,62E-12	2,09E+10		1250	1,70E-10	22578,3		25000	4,99E-11	21132,9		400000	2,38E-12	17319,9	
	100	8,62E-12	2,09E+10		1500	1,57E-10	22542		30000	4,49E-11	20671		480000	2,37E-12	17713,9	
	100	8,62E-12	2,09E+10		1875	1,42E-10	22491,9		32000	4,32E-11	20494,7		500000	2,40E-12	17816,4	
	100	8,62E-12	2,09E+10		2000	1,38E-10	22475,8		37500	3,87E-11	20029		600000	2,55E-12	18311,5	
	100	2,82E-10	22834,2		2400	1,25E-10	22416,3		40000	3,67E-11	19832,2		640000	2,61E-12	18501,6	
	120	3,09E-10	22839,5		2500	1,23E-10	22403,2		48000	3,15E-11	19252,6		800000	2,92E-12	19209	
	150	3,28E-10	22830		3000	1,12E-10	22344,5		50000	3,03E-11	19121,9		960000	3,17E-12	19804,8	
	200	3,24E-10	22807,2		3750	9,93E-11	22283,5		60000	2,52E-11	18564,3		1,00E+06	3,22E-12	19938,5	
	250	3,09E-10	22783,4		4000	9,61E-11	22273		75000	1,95E-11	17956,2					
	300	2,91E-10	22762,8		5000	8,71E-11	22260,8		80000	1,80E-11	17801,5					
	375	2,69E-10	22732,9		6000	8,17E-11	22285,8		96000	1,40E-11	17410,5					
	400	2,59E-10	22725,6		7500	7,82E-11	22357,5		100000	1,32E-11	17348,2					
	480	2,42E-10	22702,3		8000	7,72E-11	22381,7		120000	1,02E-11	17042,7					

Capacitive and resistive measurements set 4 with SiC layer above the electrodes with full sweep

BEGIN_HEADER																
	ICCAP_INPUTS															
!	<Name>	<Mode>	<+	Node>	<-	Node>	<Unit>	<Compliance>	<Sweep-type>	<Ratio>	<Offset>	<Master	Sweep>			
	Cval	V	DEFAULT	GROUND	DEFAULT	0	SYNC	1	0	Freq						
!	<Name>	<Mode>	<+	Node>	<-	Node>	<Unit>	<Compliance>	<Sweep-type>	<Ratio>	<Offset>	<Master	Sweep>			
	Gval	V	DEFAULT	GROUND	DEFAULT	0	SYNC	1	0	Freq						
!	<Name>	<Mode>	<+	Node>	<-	Node>	<Unit>	<Compliance>	<Sweep-type>	<Sweep	Order>	<Start>	<Stop>	<#	of	Points>
	Freq	V	DEFAULT	GROUND	DEFAULT	0	LIN	1	0	0	71	0				
	ICCAP_OUTPUTS															
END_HEADER																
BEGIN_DB																
	Freq	Cval	Gval		Freq	Cval	Gval		Freq	Cval	Gval		Freq	Cval	Gval	
	100	8,62E-12	2,09E+10		500	-1,83E-13	1,11E+11		5000	-1,73E-13	-1,36E+09		80000	-9,97E-14	-5,72E+07	
	100	8,62E-12	2,09E+10		600	-1,83E-13	2,12E+11		6000	-1,70E-13	-9,88E+08		96000	-9,58E-14	-4,78E+07	
	100	8,62E-12	2,09E+10		750	-1,82E-13	-4,52E+10		7500	-1,65E-13	-6,71E+08		100000	-9,52E-14	-4,58E+07	
	100	8,62E-12	2,09E+10		800	-1,81E-13	-5,91E+10		8000	-1,63E-13	-6,12E+08		120000	2,31E-15	1,40E+08	
	100	8,62E-12	2,09E+10		1000	-1,81E-13	-7,37E+10		10000	-1,57E-13	-4,38E+08		125000	2,02E-15	1,31E+08	
	100	8,62E-12	2,09E+10		1200	-1,81E-13	-2,85E+10		12000	-1,51E-13	-3,46E+08		160000	-1,08E-15	1,01E+08	
	100	8,62E-12	2,09E+10		1250	-1,82E-13	-3,34E+10		15000	-1,43E-13	-2,64E+08		200000	-6,10E-15	1,02E+08	
	100	8,62E-12	2,09E+10		1500	-1,82E-13	-1,40E+10		16000	-1,41E-13	-2,46E+08		250000	-1,05E-14	1,19E+08	
	100	8,62E-12	2,09E+10		1875	-1,80E-13	-7,98E+09		20000	-1,33E-13	-1,97E+08		300000	-1,15E-14	1,15E+08	
	100	8,62E-12	2,09E+10		2000	-1,78E-13	-8,60E+09		24000	-1,27E-13	-1,67E+08		320000	-1,16E-14	1,13E+08	
	100	-2,25E-13	-6,29E+11		2400	-1,80E-13	-6,18E+09		25000	-1,26E-13	-1,61E+08		400000	-1,06E-14	8,56E+07	
	120	-2,37E-13	-7,56E+10		2500	-1,78E-13	-4,81E+09		30000	-1,21E-13	-1,38E+08		480000	-9,14E-15	6,53E+07	
	150	-2,14E-13	5,43E+10		3000	-1,77E-13	-3,75E+09		32000	-1,19E-13	-1,31E+08		500000	-6,41E-15	4,72E+07	
	200	-1,84E-13	-4,01E+11		3750	-1,76E-13	-2,29E+09		37500	-1,16E-13	-1,15E+08		600000	1,02E-12	20009,7	
	250	-1,66E-13	-8,00E+10		4000	-1,75E-13	-2,13E+09		40000	-1,14E-13	-1,08E+08		640000	1,15E-12	20335,7	
	300	-1,91E-13	7,48E+10		2500	-1,78E-13	-4,81E+09		48000	-1,10E-13	-9,31E+07		800000	1,66E-12	21499,7	
	375	-1,94E-13	-2,89E+11		3000	-1,77E-13	-3,75E+09		50000	-1,09E-13	-8,99E+07		960000	2,06E-12	22477,8	
	400	-1,77E-13	6,27E+11		3750	-1,76E-13	-2,29E+09		60000	-1,05E-13	-7,60E+07		1,00E+06	2,14E-12	22698,3	
	480	-1,86E-13	-2,21E+11		4000	-1,75E-13	-2,13E+09		75000	-1,01E-13	-6,11E+07					

Impedance and theta measurements set 1 with SiC layer above the electrodes with full sweep

BEGIN_HEADER																
	ICCAP_INPUTS															
!	<Name>	<Mode>	<+	Node>	<-	Node>	<Unit>	<Compliance>	<Sweep-type>	<Ratio>	<Offset>	<Master	Sweep>			
	Cval	V	DEFAULT	GROUND	DEFAULT	0	SYNC	1	0	Freq						
!	<Name>	<Mode>	<+	Node>	<-	Node>	<Unit>	<Compliance>	<Sweep-type>	<Ratio>	<Offset>	<Master	Sweep>			
	Gval	V	DEFAULT	GROUND	DEFAULT	0	SYNC	1	0	Freq						
!	<Name>	<Mode>	<+	Node>	<-	Node>	<Unit>	<Compliance>	<Sweep-type>	<Sweep	Order>	<Start>	<Stop>	<#	of	Points>
	Freq	V	DEFAULT	GROUND	DEFAULT	0	LIN	1	0	0	71	0				
	ICCAP_OUTPUTS															
END_HEADER																
BEGIN_DB																
	Freq	Cval	Gval		Freq	Cval	Gval		Freq	Cval	Gval		Freq	Cval	Gval	
	100	8,62E-12	2,09E+10		500	25081	-1,187		10000	24382,7	-6,19218		125000	18056,6	-10,1451	
	100	8,62E-12	2,09E+10		600	25046	-1,33		12000	24308,8	-7,06017		160000	17689,6	-9,40609	
	100	8,62E-12	2,09E+10		750	25002	-1,533		15000	24082,6	-8,0125		200000	17491,2	-8,91881	
	100	8,62E-12	2,09E+10		800	24989	-1,592		16000	23992,2	-8,26928		250000	17416,2	-8,74777	
	100	8,62E-12	2,09E+10		1000	24931	-1,821		20000	23591,9	-9,25377		300000	17435,2	-8,9891	
	100	8,62E-12	2,09E+10		1200	24886	-2,037		24000	23182,6	-10,0786		320000	17453	-9,18583	
	100	8,62E-12	2,09E+10		1250	24874	-2,086		25000	23077,8	-10,2688		400000	17579,3	-10,2768	
	100	8,62E-12	2,09E+10		1500	24814	-2,295		30000	22547,5	-11,027		480000	17725,3	-11,7601	
	100	8,62E-12	2,09E+10		1875	24733	-2,553		32000	22336,9	-11,2939		500000	17758,4	-12,2241	
	100	8,62E-12	2,09E+10		2000	24712	-2,625		37500	21791,8	-11,7642		600000	17890,2	-14,643	
	100	25199	-0,214288		2400	24638	-2,818		40000	21561,9	-11,8917		640000	17928,6	-15,6367	
	120	25226,1	-0,300946		2500	24621	-2,862		48000	20872	-12,1332		800000	17906,9	-20,2046	
	150	25229,7	-0,42108		3000	24540	-3,069		50000	20712,3	-12,1655		960000	17662,4	-24,8517	
	200	25212,2	-0,583752		3750	24444	-3,335		60000	20034,4	-12,1135		1,00E+06	17577	-25,9671	
	250	25189,5	-0,723694		4000	24424	-3,425		75000	19286,4	-11,7645					
	300	25166,1	-0,83925		5000	24376	-3,802		80000	19095,7	-11,5902					
	375	25129	-0,995729		6000	24369	-4,205		96000	18603,7	-11,0302					
	400	25119,7	-1,03044		7500	24397	-4,933		100000	18533,3	-10,8644					
	480	25087,4	-1,16122		8000	24411	-5,18		120000	18130,2	-10,2917					

Impedance and theta measurements set 2 with SiC layer above the electrodes with full sweep

BEGIN_HEADER																
	ICCAP_INPUTS															
!	<Name>	<Mode>	<+	Node>	<-	Node>	<Unit>	<Compliance>	<Sweep-type>	<Ratio>	<Offset>	<Master	Sweep>			
	Cval	V	DEFAULT	GROUND	DEFAULT	0	SYNC	1	0	Freq						
!	<Name>	<Mode>	<+	Node>	<-	Node>	<Unit>	<Compliance>	<Sweep-type>	<Ratio>	<Offset>	<Master	Sweep>			
	Gval	V	DEFAULT	GROUND	DEFAULT	0	SYNC	1	0	Freq						
!	<Name>	<Mode>	<+	Node>	<-	Node>	<Unit>	<Compliance>	<Sweep-type>	<Sweep	Order>	<Start>	<Stop>	<#	of	Points>
	Freq	V	DEFAULT	GROUND	DEFAULT	0	LIN	1	0	0	71	0				
	ICCAP_OUTPUTS															
END_HEADER																
BEGIN_DB																
	Freq	Cval	Gval		Freq	Cval	Gval		Freq	Cval	Gval		Freq	Cval	Gval	
	100	8,62E-12	2,09E+10		500	2,87E+09	-83,57		10000	3,28E+08	-51,3411		125000	1,32E+07	111,008	
	100	8,62E-12	2,09E+10		600	2,36E+09	-82,14		12000	3,08E+08	-48,7691		160000	1,10E+07	112,104	
	100	8,62E-12	2,09E+10		750	2,06E+09	-81,07		15000	2,91E+08	-45,8963		200000	1,72E+07	132,973	
	100	8,62E-12	2,09E+10		800	1,90E+09	-81,36		16000	2,85E+08	-44,9917		250000	1,10E+07	126,604	
	100	8,62E-12	2,09E+10		1000	1,53E+09	-77,61		20000	5,68E+07	106,881		300000	7,06E+06	113,889	
	100	8,62E-12	2,09E+10		1200	1,32E+09	-74,18		24000	7,52E+07	110,646		320000	1,35E+07	139,881	
	100	8,62E-12	2,09E+10		1250	1,31E+09	-74,29		25000	4,79E+07	107,262		400000	1,21E+07	143,826	
	100	8,62E-12	2,09E+10		1500	1,15E+09	-72,5		30000	4,14E+07	107,41		480000	6,49E+06	127,587	
	100	8,62E-12	2,09E+10		1875	9,53E+08	-69,04		32000	3,94E+07	107,495		500000	5,00E+06	113,404	
	100	8,62E-12	2,09E+10		2000	9,00E+08	-68,72		37500	3,47E+07	107,585		600000	4,42E+06	112,86	
	100	1,50E+10	-73,5238		2400	7,82E+08	-66,59		40000	3,29E+07	107,664		640000	4,24E+06	112,511	
	120	1,54E+10	-89,7539		2500	7,58E+08	-66,58		48000	2,84E+07	107,784		800000	3,65E+06	111,357	
	150	1,64E+10	-81,564		3000	6,64E+08	-64,63		50000	2,75E+07	107,802		960000	3,22E+06	110,051	
	200	6,40E+09	-90,6563		3750	5,68E+08	-62,32		60000	2,37E+07	108,158		1,00E+06	3,13E+06	109,813	
	250	5,45E+09	-92,4973		4000	5,41E+08	-61,41		75000	1,97E+07	108,846					
	300	5,12E+09	-91,4705		5000	4,69E+08	-59,05		80000	1,87E+07	109,046					
	375	4,05E+09	-87,2522		6000	4,19E+08	-57,52		96000	1,62E+07	109,801					
	400	3,65E+09	-90,4448		7500	3,73E+08	-54,94		100000	1,56E+07	109,963					
	480	2,95E+09	-88,4276		8000	3,59E+08	-53,96		120000	1,36E+07	110,792					

Impedance and theta measurements set 3 with SiC layer above the electrodes with full sweep

BEGIN_HEADER																
	ICCAP_INPUTS															
!	<Name>	<Mode>	<+	Node>	<-	Node>	<Unit>	<Compliance>	<Sweep-type>	<Ratio>	<Offset>	<Master	Sweep>			
	Cval	V	DEFAULT	GROUND	DEFAULT	0	SYNC	1	0	Freq						
!	<Name>	<Mode>	<+	Node>	<-	Node>	<Unit>	<Compliance>	<Sweep-type>	<Ratio>	<Offset>	<Master	Sweep>			
	Gval	V	DEFAULT	GROUND	DEFAULT	0	SYNC	1	0	Freq						
!	<Name>	<Mode>	<+	Node>	<-	Node>	<Unit>	<Compliance>	<Sweep-type>	<Sweep	Order>	<Start>	<Stop>	<#	of	Points>
	Freq	V	DEFAULT	GROUND	DEFAULT	0	LIN	1	0	0	71	0				
	ICCAP_OUTPUTS															
END_HEADER																
BEGIN_DB																
	Freq	Cval	Gval		Freq	Cval	Gval		Freq	Cval	Gval		Freq	Cval	Gval	
	100	8,62E-12	2,09E+10		500	22704	-0,966		10000	22237,9	-5,92589		125000	16854,3	-7,24417	
	100	8,62E-12	2,09E+10		600	22681	-1,081		12000	22105,2	-6,65154		160000	16649	-6,23284	
	100	8,62E-12	2,09E+10		600	22653	-1,253		15000	21851,8	-7,52252		200000	16595,3	-5,47251	
	100	8,62E-12	2,09E+10		750	22646	-1,303		16000	21755,6	-7,75483		250000	16667,4	-4,99984	
	100	8,62E-12	2,09E+10		800	22610	-1,497		20000	21353,3	-8,61208		300000	16823,8	-4,98388	
	100	8,62E-12	2,09E+10		1000	22584	-1,681		24000	20952,9	-9,25673		320000	16896,4	-5,09005	
	100	8,62E-12	2,09E+10		1250	22575	-1,725		25000	20853,4	-9,39873		400000	17231,4	-5,89927	
	100	8,62E-12	2,09E+10		1500	22536	-1,911		30000	20365,9	-9,92563		480000	17577,3	-7,20878	
	100	8,62E-12	2,09E+10		1875	22482	-2,157		32000	20182	-10,1002		500000	17662,1	-7,64083	
	100	8,62E-12	2,09E+10		2000	22465	-2,228		37500	19707,8	-10,3433		600000	18038,1	-9,98848	
	100	22849,2	-0,232597		2400	22402	-2,425		40000	19511,6	-10,3787		640000	18167,2	-10,9839	
	120	22851	-0,305274		2500	22389	-2,472		48000	18942,9	-10,3538		800000	18494,2	-15,7323	
	150	22841,3	-0,404425		3000	22327	-2,691		50000	18815,5	-10,325		960000	18525,6	-20,754	
	200	22818,7	-0,532015		3750	22260	-2,983		60000	18284,3	-10,0148		1,00E+06	18496	-21,982	
	250	22794,4	-0,632748		4000	22247	-3,079		75000	17718,3	-9,38603					
	300	22772	-0,71363		5000	22228	-3,486		80000	17578	-9,14202					
	375	22741,2	-0,825578		6000	22240	-3,927		96000	17226,5	-8,39237					
	400	22733,2	-0,847578		7500	22289	-4,709		100000	17173,5	-8,19015					
	480	22707,7	-0,946707		8000	22306	-4,97		120000	16902	-7,42967					

Impedance and theta measurements set 4 with SiC layer above the electrodes with full sweep

BEGIN_HEADER																
	ICCAP_INPUTS															
!	<Name>	<Mode>	<+	Node>	<-	Node>	<Unit>	<Compliance>	<Sweep-type>	<Ratio>	<Offset>	<Master	Sweep>			
	Cval	V	DEFAULT	GROUND	DEFAULT	0	SYNC	1	0	Freq						
!	<Name>	<Mode>	<+	Node>	<-	Node>	<Unit>	<Compliance>	<Sweep-type>	<Ratio>	<Offset>	<Master	Sweep>			
	Gval	V	DEFAULT	GROUND	DEFAULT	0	SYNC	1	0	Freq						
!	<Name>	<Mode>	<+	Node>	<-	Node>	<Unit>	<Compliance>	<Sweep-type>	<Sweep	Order>	<Start>	<Stop>	<#	of	Points>
	Freq	V	DEFAULT	GROUND	DEFAULT	0	LIN	1	0	0	71	0				
	ICCAP_OUTPUTS															
END_HEADER																
BEGIN_DB																
	Freq	Cval	Gval		Freq	Cval	Gval		Freq	Cval	Gval		Freq	Cval	Gval	
	100	8,62E-12	2,09E+10		500	22704	-0,98		10000	22503	-5,37526		125000	17277,3	-5,18742	
	100	8,62E-12	2,09E+10		600	22678	-1,086		12000	22372,7	-6,00074		160000	17135,5	-3,70045	
	100	8,62E-12	2,09E+10		750	22648	-1,241		15000	22139,5	-6,78		200000	17167,4	-2,42763	
	100	8,62E-12	2,09E+10		800	22640	-1,285		16000	22049,7	-6,99347		250000	17366,8	-1,37423	
	100	8,62E-12	2,09E+10		1000	22603	-1,455		20000	21674,1	-7,81859		300000	17672,5	-0,847823	
	100	8,62E-12	2,09E+10		1200	22577	-1,615		24000	21296,5	-8,44089		320000	17811,4	-0,767943	
	100	8,62E-12	2,09E+10		1250	22568	-1,651		25000	21200,8	-8,57512		400000	18430,7	-0,958952	
	100	8,62E-12	2,09E+10		1500	22530	-1,805		30000	20723,7	-9,06889		480000	19083,1	-1,82637	
	100	8,62E-12	2,09E+10		1875	22476	-2,001		32000	20542	-9,23353		500000	19249,3	-2,17091	
	100	8,62E-12	2,09E+10		2000	22460	-2,054		37500	20070,3	-9,43267		600000	20029,3	-4,23333	
	100	22829,3	-0,195859		2400	22397	-2,193		40000	19873,2	-9,44758		640000	20315,6	-5,17306	
	120	22838,3	-0,270492		2500	22386	-2,225		48000	19301,2	-9,34628		800000	21241,8	-10,0102	
	150	22835,1	-0,375615		3000	22346	-2,37		50000	19173,3	-9,29386		960000	21741,7	-15,4694	
	200	22815,2	-0,51452		3750	22324	-2,586		60000	18643,7	-8,86031		1,00E+06	21804,8	-16,8329	
	250	22794,7	-0,627776		4000	22329	-2,663		75000	18083,5	-8,02864					
	300	22773,2	-0,7187		5000	22379	-3,059		80000	17947,4	-7,71623					
	375	22742,4	-0,839529		6000	22462	-3,525		96000	17612,3	-6,74402					
	400	22733,7	-0,863268		7500	22592	-4,329		100000	17561	-6,48185					
	480	22708,5	-0,96188		8000	22609	-4,557		120000	17317,3	-5,43982					

Bibliography

[1] S. E. Lewis, J. R. DeBoer, J. L. Gole, and P. J. Hesketh, *Sensitive, selective, and analytical improvements to a porous silicon gas sensor,* Sensors and Actuators B: Chemical **110**, 54 (2005).

[2] B. Timmer, W. Olthuis, and A. Van Den Berg, *Ammonia sensors and their applications—a review,* Sensors and Actuators B: Chemical **107**, 666 (2005).

[3] C. Harris, S. Savage, A. Konstantinov, M. Bakowski, and P. Ericsson, *Progress towards sic products,* Applied Surface Science **184**, 393 (2001).

[4] R. Bogue, *Mems sensors: past, present and future,* Sensor Review **27**, 7 (2007).

[5] A. L. Spetz, J. Huotari, C. Bur, R. Bjorklund, J. Lappalainen, H. Jantunen, A. Schütze, and M. Andersson, *Chemical sensor systems for emission control from combustions,* Sensors and Actuators B: Chemical **187**, 184 (2013).

[6] X. Liu, S. Cheng, H. Liu, S. Hu, D. Zhang, and H. Ning, *A survey on gas sensing technology,* Sensors **12**, 9635 (2012).

[7] Z. Yunusa, M. N. Hamidon, A. Kaiser, and Z. Awang, *Gas sensors: a review,* Sensors & Transducers **168**, 61 (2014).

[8] *SOLID STATE GAS SENSORS: state of the art and future activities,* https://joam.inoe.ro/arhiva/pdf5_5/Capone.pdf.

[9] A. Azad, S. Akbar, S. Mhaisalkar, L. Birkefeld, and K. Goto, *Solid-state gas sensors: A review,* Journal of the Electrochemical Society **139**, 3690 (1992).

[10] N. Wright and A. Horsfall, *Sic sensors: a review,* Journal of Physics D: Applied Physics **40**, 6345 (2007).

[11] M. Mehregany and C. A. Zorman, *Sic mems: opportunities and challenges for applications in harsh environments,* Thin solid films **355**, 518 (1999).

[12] *SiC applications nasa description,* https://sic.grc.nasa.gov.

[13] A. Betser, *A photoelastic study of maximum tensile stresses in simply supported short beams under central transverse impact,* in *Photoelasticity* (Elsevier, 1969) pp. 319–331.

[14] G. T. Kovacs *et al.*, *Micromachined transducers sourcebook,* (1998).

[15] J. F. Shackelford, Y.-H. Han, S. Kim, and S.-H. Kwon, *CRC materials science and engineering handbook* (CRC press, 2016).

[16] M. Lord and A. James, *Macmillan's chemical and physical data,* (1992).

[17] A. Bailey, E. Gilham, E. Herington, and B. Rose, *Kaye and laby'tables of physical and chemical constants,* (1973).

[18] C. J. Smithells and E. A. Brandes, *Metals reference book*, Vol. 860 (Butterworths, London Boston, 1976).

[19] C. Klingsberg, *The physics and chemistry of ceramics: proceedings of a symposium held at the Pennsylvania State University, May 28-30, 1962* (Gordon and Breach, 1963).

[20] M. A. LaBarbera, *Long-Term, High Temperature Mechanical Stability of PECVD Amorphous Silicon Carbide for Use as Structural Material in Harsh Environment MEMS*, Ph.D. thesis, Case Western Reserve University (2014).

[21] X.-A. Fu, J. L. Dunning, C. A. Zorman, and M. Mehregany, *Polycrystalline 3c-sic thin films deposited by dual precursor lpcvd for mems applications,* Sensors and actuators A: Physical **119**, 169 (2005).

[22] B. Cros, E. Gat, and J. Saurel, *Characterization of the elastic properties of amorphous silicon carbide thin films by acoustic microscopy,* Journal of non-crystalline solids **209**, 273 (1997).

[23] M. El Khakani, M. Chaker, A. Jean, S. Boily, J. Kieffer, M. O'hern, M. Ravet, and F. Rousseaux, *Hardness and young's modulus of amorphous a-sic thin films determined by nanoindentation and bulge tests,* Journal of materials research **9**, 96 (1994).

[24] J. B. Birks, *Modern dielectric materials,* (1960).

[25] R. Speyer, *Thermal analysis of materials* (CRC press, 1993).

[26] K. M. Jackson, *Fracture strength, elastic modulus and poisson's ratio of polycrystalline 3c thin-film silicon carbide found by microsample tensile testing,* Sensors and Actuators A: Physical **125**, 34 (2005).

[27] K. Tolpygo, *The present state of the theory of polarization of ideal ionic and valence crystals,* Physics-Uspekhi **4**, 485 (1961).

[28] J. Vlassak and W. Nix, *A new bulge test technique for the determination of young's modulus and poisson's ratio of thin films,* Journal of Materials Research **7**, 3242 (1992).

[29] M. T. Kim, *Influence of substrates on the elastic reaction of films for the microindentation tests,* Thin Solid Films **283**, 12 (1996).

[30] K. E. Petersen, *Silicon as a mechanical material,* Proceedings of the IEEE **70**, 420 (1982).

[31] *MS Windows NT kernel description,* https://www.washingtonmills.com/history-of-silicon-carbide/sic-properties/.

[32] J. Bullot and M. Schmidt, *Physics of amorphous silicon–carbon alloys,* physica status solidi (b) **143**, 345 (1987).

[33] V. Ivashchenko, P. E. Turchi, V. Shevchenko, L. Ivashchenko, and G. Rusakov, *Tight-binding-molecular-dynamics investigation of the atomic and electronic structure properties of ac, a-si and a-sic,* Diamond and related materials **12**, 993 (2003).

[34] D. McCulloch, A. Merchant, N. Marks, N. Cooper, P. Fitzhenry, M. Bilek, and D. McKenzie, *Wannier function analysis of tetrahedral amorphous networks,* Diamond and related materials **12**, 2026 (2003).

[35] A. Lloyd, P. Tobias, A. Baranzahi, P. Martensson, and I. Lundstrom, *Current status of silicon carbide based high-temperature gas sensors,* IEEE Transactions on Electron Devices **46**, 561 (1999).

[36] *Porous Silicon in Practice: preparation, characterization and applications description,* https://application.wiley-vch.de/books/sample/3527313788_c01.pdf.

[37] S. Ozdemir and J. L. Gole, *The potential of porous silicon gas sensors,* Current Opinion in Solid State and Materials Science **11**, 92 (2007).

[38] C. Pijolat, C. Pupier, M. Sauvan, G. Tournier, and R. Lalauze, *Gas detection for automotive pollution control,* Sensors and Actuators B: Chemical **59**, 195 (1999).

[39] T. D. Durbin, R. D. Wilson, J. M. Norbeck, J. W. Miller, T. Huai, and S. H. Rhee, *Estimates of the emission rates of ammonia from light-duty vehicles using standard chassis dynamometer test cycles,* Atmospheric Environment **36**, 1475 (2002).

[40] M. Wallin, C.-J. Karlsson, M. Skoglundh, and A. Palmqvist, *Selective catalytic reduction of nox with nh3 over zeolite h–zsm-5: influence of transient ammonia supply,* Journal of Catalysis **218**, 354 (2003).

[41] A. T. Bulgan, *Use of low temperature energy sources in aqua-ammonia absorption refrigeration systems,* Energy conversion and management **38**, 1431 (1997).

[42] P. Colonna and S. Gabrielli, *Industrial trigeneration using ammonia–water absorption refrigeration systems (aar),* Applied Thermal Engineering **23**, 381 (2003).

[43] R. K. Srivastava, P. Lal, R. Dwivedi, and S. Srivastava, *Sensing mechanism in tin oxide-based thick-film gas sensors,* Sensors and Actuators B: Chemical **21**, 213 (1994).

[44] H.-P. Hübner and S. Drost, *Tin oxide gas sensors: an analytical comparison of gas-sensitive and non-gas-sensitive thin films,* Sensors and Actuators B: Chemical **4**, 463 (1991).

[45] K. Zakrzewska, *Mixed oxides as gas sensors,* Thin solid films **391**, 229 (2001).

[46] F. Winquist, A. Spetz, I. Lundström, and B. Danielsson, *Determination of ammonia in air and aqueous samples with a gas-sensitive semiconductor capacitor,* Analytica chimica acta **164**, 127 (1984).

[47] I. Lundström, A. Spetz, F. Winquist, U. Ackelid, and H. Sundgren, *Catalytic metals and field-effect devices—a useful combination,* Sensors and Actuators B: Chemical **1**, 15 (1990).

[48] N. Mayo, R. Harth, U. Mor, D. Marouani, J. Hayon, and A. Bettelheim, *Electrochemical response to h2, o2, co2 and nh3 of a solid-state cell based on a cation-or anion-exchange membrane serving as a solid polymer electrolyte,* Analytica chimica acta **310**, 139 (1995).

[49] I. Lähdesmäki, W. W. Kubiak, A. Lewenstam, and A. Ivaska, *Interferences in a polypyrrole-based amperometric ammonia sensor,* Talanta **52**, 269 (2000).

[50] E. Palmqvist, C. B. Kriz, K. Svanberg, M. Khayyami, and D. Kriz, *Dc-resistometric urea sensitive device utilizing a conducting polymer film for the gas-phase detection of ammonia,* Biosensors and Bioelectronics **10**, 283 (1995).

[51] A. Ghauch, J. Rima, A. Charef, J. Suptil, C. Fachinger, and M. Martin-Bouyer, *Quantitative measurements of ammonium, hydrogenophosphate and cu (ii) by diffuse reflectance spectrometry,* Talanta **48**, 385 (1999).

[52] P. L. Searle, *The berthelot or indophenol reaction and its use in the analytical chemistry of nitrogen. a review,* Analyst **109**, 549 (1984).

[53] R. Memming, *Semiconductor electrochemistry* (2012).

[54] *SiC etch: pec etch description,* http://www.nnin.org/sites/default/files/files/2007nninREUbabb.pdf.